The use of geosynthetics in roads

J.P. Giroud[1], J. Han[2], E. Tutumluer[3] and M.J.D. Dobie[4]

[1]*Consulting Engineer, Paris, France, E-mail: jpg@jpgiroud.com (corresponding author)*
[2]*Professor, The University of Kansas, Lawrence, Kansas, USA, E-mail: jiehan@ku.edu*
[3]*Professor, The University of Illinois at Urbana-Champaign, Urbana, IL, USA, E-mail: tutumlue@illinois.edu*
[4]*Regional Manager Asia Pacific, Tensar International, Menara Sentraya, Jakarta, Indonesia, E-mail: mdobie@tensar.co.id*

Received 23 December 2020, accepted 18 October 2021, published 17 March 2022

ABSTRACT: This paper addresses unpaved and paved roads improved with geosynthetics, such as geotextiles, geogrids and geocells. The paper examines the mechanisms associated with the use of geosynthetics to improve roads, describes the principles of the design methods used to quantify the benefits of geosynthetics used in unpaved and paved roads, presents case histories to demonstrate the use of geosynthetics to solve challenging road problems, and discusses the relevance of tests and trials to real roads. This paper is supplemented by four presentations in pdf format that contain more than 800 slides. These four presentations are updated versions of the four presentations made during a one-day short course at the 11th International Conference on Geosynthetics held in Seoul, Korea, in September 2018. The paper that follows contains a summary of each of the four presentations, with special emphasis on key issues.

KEYWORDS: Geosynthetics, geotextiles, geogrids, geocells, roads, paved, unpaved, pavements, traffic, loads, functions, mechanisms

REFERENCE: Giroud, J.P., Han, J., Tutumluer, E. and Dobie, M.J.D. (2023). The use of geosynthetics in roads. *Geosynthetics International*, **30**, No. 1, 47–80. [https://doi.org/10.1680/jgein.21.00046]

1. INTRODUCTION

1.1. Overview

Geosynthetics have drastically changed the way roads are designed and constructed. Early applications were limited uses of cotton fabrics in paved roads in the 1930s and uses of fabrics in the 1940s in World War II to facilitate military equipment traffic. However, the first major step of the modern development of the use of geosynthetics in roads was the use of nonwoven fabrics (not yet called geotextiles) in the late 1960s to successfully construct access roads at construction sites where driving trucks was otherwise impossible. The second major step in the development of the use of geosynthetics in roads was the advent of geogrids in the 1980s. It can be expected that there will be other major steps in the future, perhaps related to the development of new geosynthetics or to the growing use in roads of existing geosynthetics such as geocells.

Geosynthetics have brought an impulse of innovation to road construction, one of the most traditional and basic construction activities. This impulse of innovation is now materialized by the variety of geosynthetics used in road applications. The geosynthetics currently used in roads include: geotextiles (woven and nonwoven), geogrids with different geometries, geocells, drainage geocomposites, wicking geotextiles, and so on. There are even a few examples of uses of geomembranes in roads. These geosynthetics perform a number of functions as discussed in Section 2.1.2. As a result, geosynthetics are highly beneficial to roads by providing better performance and increased service life. Alternatively, geosynthetics can be used to allow a smaller thickness of the road cross-section or the use of lower quality construction materials.

In addition to their beneficial impact on road design and performance, geosynthetics facilitate road construction in a number of cases. There are even cases where the subgrade is so soft that it would be impossible to start construction of a road without first placing a geosynthetic on the subgrade (see Slides A.435 to A.451 in Presentation A that appears in the Supplemental Material to this paper).

1.2. Road structure and terminology

1.2.1. *Unpaved roads*

A typical cross-section of an unpaved road incorporating a geosynthetic is shown in Figure 1. The base course is typically made of aggregate. In most cases, the geosynthetic is a geogrid or a geotextile. The geogrid or the geotextile is typically placed between the base course and

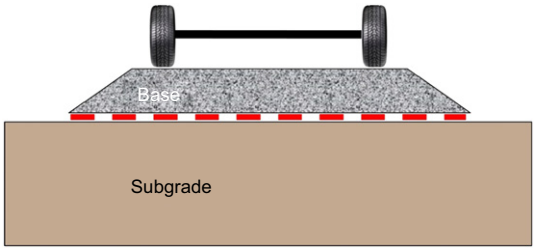

Figure 1. Cross-section of a typical unpaved road incorporating a geosynthetic between base and subgrade

the subgrade (as shown in Figure 1). In some cases, the geosynthetic is a geocell. In those cases, the lower part of the base material is contained within the geocell (see Slides A.22 to A.25). Typical photos of unpaved roads can be seen in Slides A.13 to A.23.

1.2.2. *Paved roads*

A typical cross-section of a paved road incorporating a geosynthetic is shown in Figure 2 for the case of an asphalt surface course and Figure 3 for the case of a concrete surface course. Paved roads with asphalt surface course are commonly referred to as 'flexible pavements' (and sometimes as 'asphalt pavements') whereas paved roads with concrete surface course are commonly referred to as 'rigid pavements' (and sometimes as 'concrete pavements'). The term 'conventional flexible pavement' refers to a pavement

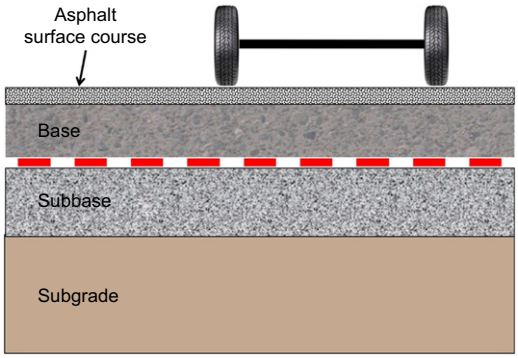

Figure 2. Cross-section of a typical paved road, with asphalt surface course, incorporating a geosynthetic between base and subbase. Note: Other configurations are possible with geosynthetic between subbase and subgrade, and/or geosynthetic used to reinforce the asphalt surface course.

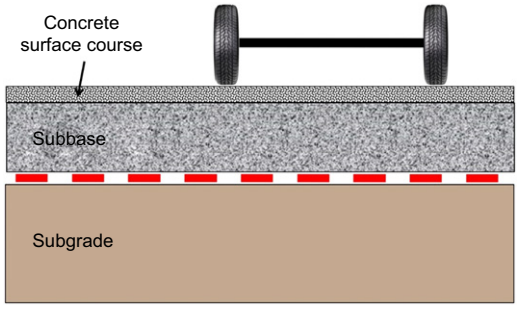

Figure 3. Cross-section of a typical paved road, with concrete surface course, incorporating a geosynthetic between subbase and subgrade

comprising the following components from top to bottom: asphalt surface course, unbound base, unbound subbase (optional), and compacted subgrade. A conventional flexible pavement can be improved by inclusion of one or more layers of geosynthetics.

In the case of paved roads with asphalt surface course, the base course is commonly made of (1) unbound aggregate, (2) cement-treated soil or aggregate, or (3) asphalt-treated soil or aggregate; however, it can be made of other materials. Aggregate is generally crushed stone. The subbase is often made of materials of lesser quality than the materials used in the base course. In the case of paved roads with concrete surface course, there is typically a subbase, but there is typically no base course (as shown in Figure 3) because the rigidity of the concrete surface course is sufficient to distribute the wheel loads without the need for a base course.

1.2.3. *Traffic quantification*

The concept of equivalent traffic

Traffic can be quantified by the number of passes of vehicles. However, to compare the passes of different vehicles having different axle loads and numbers of axles, traffic is expressed in terms of number of passes of a standard axle load equivalent to the number of passes of the considered vehicles. The standard axle load used in the United States is 80 kN. (In AASHTO (1993), this standard axle load is expressed as 18 kips (kilopounds), which is the same as 80 kN in SI units.) The standard axle load may be different in different countries. Therefore, when an equivalent number of passes of a standard axle is mentioned, it is necessary to indicate what standard axle load is used.

The practice in the United States consists in calling ESAL (Equivalent Single Axle Load) the number of passes of an 80 kN axle that is equivalent to the number of passes of the considered vehicles. Therefore, even though the acronym ESAL implies that it is a load, the term ESAL is used (sometimes in the plural form, ESALs) as a way to quantify a number of passes.

Determination of the equivalent traffic

Using equal fatigue failure of asphalt pavement as a criterion for equivalency between the actual traffic and the standard axle traffic has led to the following equation to determine the ESAL count (Deacon *et al.* 1969):

$$\mathrm{ESAL} = N_{\mathrm{actual}} \left(\frac{P_{\mathrm{actual}}}{P_{\mathrm{standard}}} \right)^4 \qquad (1)$$

where ESAL is the standard axle's number of passes that is equivalent to the number of passes of the actual axles; N_{actual} is the number of passes of the actual axles; P_{actual} is the actual axle load; and P_{standard} is the standard axle load (80 kN in the United States). Guidance for the use of Equation (1) in the case of vehicles comprising several axles with different loads can be found in Appendix I of the paper by Giroud and Noiray (1981).

In the case of unpaved roads, Sun *et al.* (2015), using equal permanent deformations for the equivalency criterion, showed that, for actual axle loads lower than

80 kN, Equation (1) could be used with an exponent between 1.9 and 2.9 depending on base thickness, presence of geogrid, and properties of the geogrid if any. Unpublished analyses by the fourth author of this paper have shown that an exponent between 3 and 4 can be used for unpaved roads with actual axle loads higher than 80 kN (see Slide D.77).

Another method to determine the ESAL count has been presented in successive AASHTO guides since 1972 (see AASHTO 1993). With this method, the ESAL count for mixed traffic (i.e. traffic of different axles) based on pavement performance is determined as a function of several parameters such as wheel load, structural number (which characterizes the pavement structural capacity) for asphalt pavements or slab thickness for concrete pavements, and axle type (single, tandem, tridem). The term 'tandem' refers to a group of two axles, and 'tridem' to a group of three axles. Tables provided in Huang (2004) facilitate the use of the AASHTO method.

State of practice for equivalent traffic expression and determination

The use of ESAL may be confusing for readers who are not familiar with practice of road engineers in the United States. For example, 'ESAL = 6300 (also reported as 6300 ESALs)' means that the actual number of passes of the considered axles or vehicles has been calculated to be equivalent to 6300 passes of a standard axle. Clearly, when used in this manner, ESAL quantifies a number of passes and is, therefore, dimensionless.

In the United States, the method presented in the 1993 AASHTO Design Guide is typically used to determine the equivalent traffic for asphalt and concrete pavements. However, because of its simplicity and because the method presented in the 1993 AASHTO Design Guide and Equation (1) give similar results for asphalt pavements, Equation (1) is frequently used for asphalt pavements and generally used for unpaved roads. Since there are several methods for determining the ESAL, it is important to indicate the method used to determine the ESAL every time an ESAL value is mentioned. It should be noted that an approach to quantify traffic, different from the ESAL concept, consists in using the Mechanistic-Empirical (M-E) methodology with detailed axle load spectra information. (See Section 4 where the M-E methodology is addressed.)

Magnitude of equivalent traffic

Equation (1) shows that the load ratio between the actual axles and the standard axle has a large impact on the ESAL. Thus, if the actual axle load is double the standard axle load, the ESAL is 16 times higher than the actual number of passes, if Equation (1) is used with exponent 4.

1.3. Scope of this paper

The scope of this paper is somehow unusual, because the presentations can be considered more important than the paper itself. Indeed, whereas the paper is relatively short, the presentations contain a wealth of information. The presentations that appear in the Supplemental Material to this paper are updated versions of the presentations made in a one-day short course on geosynthetic-stabilized roads presented at the 11th International Conference on Geosynthetics, held in Seoul, Korea, in September 2018, under the auspices of the International Geosynthetics Society (IGS), and organized by the Korean Chapter of the IGS, under the chairmanship of C. Yoo.

This course, organized by J. Han, was successful, with 49 pre-registered participants and 118 attendees actually present, whereas it is known that the number of actual attendees to short courses is often lower than the number of pre-registered participants. As a result of this success, the publication of a paper, with the slides available as Supplemental Material to the paper, was suggested to the course instructors. Hence this paper.

The short course included four sessions, of 90 minutes each. After the short course presentation in September of 2018, many of the slides have been improved and a number of new slides have been added. As a result, the four presentations provided with this paper are far more complete than the handout that was given to some of the attendees; and, for each of the four sessions, the provided slides would require more than 90 minutes to be presented.

The subjects, in the order of presentation, were:

- Mechanisms of Road Improvement by Geosynthetics, by J.P. Giroud, of which a summary is hereafter in Section 2, and the slides are in Presentation A;
- Design of Geosynthetic-Improved Unpaved Roads and Case Studies, by J. Han, of which a summary is hereafter in Section 3, and the slides are in Presentation B;
- Design of Geosynthetic-Improved Paved Roads and Case Studies, by E. Tutumluer, of which a summary is hereafter in Section 4, and the slides are in Presentation C; and
- Relevance of Tests and Trials to Real Roads by M. Dobie, of which a summary is hereafter in Section 5, and the slides are in Presentation D.

The four presentations appear in the Supplemental Material to this paper. The slide numbers mentioned in this paper are consistent with the numbers shown in the footers of the slides of the provided presentations. For example, 'Slide B.5' is the fifth slide of Presentation B. The four authors have endeavored to coordinate their presentations to avoid inconsistencies and to use a common terminology.

2. MECHANISMS OF ROAD IMPROVEMENT BY GEOSYNTHETICS

2.1. Functions and mechanisms of road improvement

2.1.1. *Definitions of functions and mechanisms*

What is a function and what is a mechanism? In this Section 2, the mechanisms of road improvement by geosynthetics will be discussed and, in the discussions,

the functions performed by the geosynthetics will be mentioned. In some publications, the terms 'function' and 'mechanism' are used interchangeably, which creates confusion. Therefore, definitions are necessary.

The various functions performed by geosynthetics have been discussed since the 1970s (e.g. Giroud 1977). However, whereas the term 'function' is often used, it is rarely defined in publications devoted to geosynthetics.

The mechanism-versus-function discussion is classical among philosophers. Adapting their language to engineering leads to the following tentative definitions:

- Function can be defined as the basic role played by a component of a system.
- Mechanism can be defined as a mode of interaction between the components of a system (e.g. relative displacements and forces between the components of the system) that governs the behavior of the system, where each component performs one or several functions.

The term 'geotechnical system' is used herein for systems constructed mostly using natural materials (or similar materials such as recycled concrete aggregate, reclaimed asphalt pavement aggregate, and lightweight aggregate). There are many types of geotechnical systems. A few examples are: embankments, road pavements, unpaved areas, earth dams, earth slopes, landfills, reinforced soil walls, drainage layers. In the remainder of this paper, the term 'system' will be used as a shortening for 'geotechnical system', except in a few occasions where it is appropriate to specifically use the term 'geotechnical'.

In the case of geotechnical systems incorporating geosynthetics, the following definitions can be derived from the above general definitions:

- A function of a geosynthetic is a specific role played by the geosynthetic in a geotechnical system and made possible by specific properties of the geosynthetic.
- A mechanism, associated with the performance of a geosynthetic in a geotechnical system (such as a certain type of road), is a mode of interaction (defined by forces and displacements) between the geosynthetic (performing one or several functions) and the other materials (e.g. soil particles and water) involved in the system.

In a geotechnical system such as a road, several components are included – for example subgrade soil, layers of aggregates, asphalt, concrete and geosynthetics. All components, in particular the geosynthetics, perform one or more functions. The development of mechanisms that govern the performance of a system depends on the organization of the system, which is conditioned by the geometry of the system and the interaction between the components of the system (e.g. interface friction, boundary deformation, etc.).

It should be noted that a single geosynthetic may perform different functions at the same time, or successively, and may be involved in more than one mechanism.

2.1.2. *Functions of geosynthetics in roads*

Seven functions

Geosynthetics perform more functions than the five or six functions usually mentioned, but not all geosynthetics functions are performed in roads. The geosynthetics functions performed in roads (excluding functions performed in geotechnical systems associated with roads, such as slopes and embankments) include: reinforcement, stabilization, stress-relief interlayer, separation, fluid barrier, drainage, and filtration. The order in the list of functions does not imply any hierarchy between functions. For the sake of clarity, mechanical functions are listed first, followed by functions related to water. These functions of geosynthetics are described below, with special emphasis on road applications.

In the description of functions which follows, the term 'soil' is a generic term that encompasses all particulate materials likely to be associated with geosynthetics. Examples include: natural soils, crushed aggregate, recycled concrete, reclaimed asphalt pavement, and so on.

Reinforcement function

A geosynthetic performs the reinforcement function when it increases the strength and/or reduces the deformation of a material (such as a soil or a related material such as asphalt mix) or a system by carrying tensile forces that the material alone would not carry. Reinforcement is made possible by mobilization of the appropriate level of geosynthetic tensile strength in response to the tensile forces generated in the geosynthetic as a result of interaction between the adjacent material and the geosynthetic.

Tensile forces are generated in the geosynthetic in three ways or a combination of these three ways: (1) shear stresses between the geosynthetic and the soil, as in the case of an embankment on soft soil, or shear stresses between the geosynthetic and a material to which the geosynthetic is bonded, as in the case of asphalt mix; (2) axial pull exerted directly on the geosynthetic, as in the case of a geosynthetic attached to the facing of a mechanically stabilized earth wall; and/or (3) tensile forces associated with the out-of-plane deformation of the geosynthetic due to a load approximately perpendicular to the plane of the geosynthetic, as in the case of the tensioned membrane effect in a road.

A geosynthetic subjected to tensile forces is said to be under tension. A geosynthetic under tension reinforces a material to which it is bonded by reducing its deformation and, in some cases, preventing cracking of the material. A geosynthetic under tension reinforces a system (such as a road) by linking different parts of the system, thereby reducing the system deformation and, in some cases, preventing rupture (e.g. shear failure) of the system by keeping together two parts of the system which would tend to move apart in the absence of reinforcement.

Reinforcement may occur at different scales:

- Reinforcement takes place at a small scale (i.e. the scale of intimate bonding between the geosynthetic and the material) in the case of cracking prevention. This is the case of reinforcement by a geogrid of an asphalt surface course or an asphalt overlay (see Slides A.330 to A.333, and A.346 and A.347). In this 'small scale case', it may be argued that the geosynthetic reinforces the material (e.g. the asphalt mix) as well as the system (e.g. the asphalt surface course). A typical example of reinforcement that takes place at a small scale is concrete reinforcement with steel or polymeric fibers against concrete cracking.
- Reinforcement takes place at the scale of a system (such as a road) when a geosynthetic transfers tensile forces from one place to another place where the geosynthetic is anchored. In this case, the geosynthetic reinforces the system rather than the material. Examples of reinforcement at the scale of a road structure are: the increase of the bearing capacity of the subgrade by a geosynthetic performing the reinforcement function through the subgrade heave restraint mechanism (see Section 2.2.3), and the reduction of the maximum stress on the subgrade by a geosynthetic performing the reinforcement function through the tensioned membrane effect (see Section 2.2.4).

If reinforcement takes place at a small scale, bonding between the geosynthetic and the material should be adequate. In the case of reinforcement at the scale of a system, anchorage between the geosynthetic and the material in the stable zone is essential, hence the concept of anchorage length.

Stabilization function

A geosynthetic (typically a geocell or a geogrid, and to a lesser degree a geotextile) performs the stabilization function when it forms a geosynthetic/soil composite material that is less deformable than the soil. As a result of the close interaction between the geosynthetic and the soil, the displacements of the composite material in the planar direction of the geosynthetic are significantly reduced compared to the displacements that the non-stabilized soil would have under the same loads; in other words, the displacement of the soil is restrained over the entire area where the composite material is created. Compared to the non-stabilized soil, this composite material typically has (1) a higher strength and (2) a higher modulus related to deformation under repeated loads (even though the modulus under a single load may be similar for the composite material and the non-stabilized soil). The increase in strength and modulus is sometimes referred to as 'stiffening'.

The term 'confinement' is often used in conjunction with the lateral restraint of the soil associated with the stabilization function. This is an appropriate terminology because the mechanical action of the geosynthetic, which results in lateral restraint, is equivalent to the application of a lateral confining stress, a familiar concept in geotechnical engineering.

Geocells, geogrids and geotextiles do not have the same mode of interaction with soil:

- In the case of a geocell, the soil is actually confined inside each cell of the geocell. This is described as 'closed confinement' (Slides A.68 to A.74). Confinement in a given cell of a geocell results from: (1) tension in the geosynthetic material that constitutes the walls of the cell; and (2) normal stresses applied on the walls of the cell by the surrounding cells. Confinement in a geocell is effective with any type of soil provided it is adequately compacted, whereas, in the case of a geogrid, selection of the soil is of utmost importance. The fact that any type of soil can be used in geocells makes it possible to use local soils, which has many advantages. However, placing and compacting soil inside geocells is labor intensive.
- In the case of a geogrid, the associated soil is typically aggregate, and there is interlocking between the geogrid and the aggregate particles located inside the geogrid apertures. The degree of interlocking depends on the aggregate grading. It is, therefore, possible to ensure optimum interlocking with appropriate grading of the aggregate. The layer of aggregate, which interlocks with the geogrid, interacts with the adjacent layer of aggregate and so on, as shown in Slides A.75 to A.85. While the first layer of aggregate, which is directly in contact with the geogrid, is fully confined, other layers of aggregate are progressively less confined with increasing distances from the geogrid. This mode of confinement is referred to as 'open confinement'. Also, with some types of geogrids, interaction with the aggregate may, to some degree, involve friction (see Slides A.90 to A.93). It should be noted that a geogrid provides some confinement to aggregate that does not have the appropriate grading to ensure optimum interlocking, and even provides some confinement to sand; however, maximum confinement by geogrid does require the use of aggregate that has the appropriate grading to ensure optimum interlocking with the geogrid.
- In the case of a geotextile, some confinement of the soil in contact with the geotextile may result from soil/geotextile friction. However, this is not an important mode of action of geotextiles in roads.

The thickness of the confined zone is an essential consideration in the design and the performance of a road:

- In the case of a geocell, the thickness of the confined zone is the height of the geocell. There may be some confinement in a thin layer of soil above the geocell, but this confinement is generally negligible, especially if the geocell is filled with sand or a finer soil.
- In the case of a geogrid, as explained above, the degree of confinement decreases with increasing distances from the geogrid. In this case it is possible to consider

an effective confinement thickness, which depends on the geogrid and the material being stabilized – namely the base/subbase material (see Slides A.82 to A.85). If the base or subbase thickness exceeds the effective confinement thickness, an additional layer of geogrid may be considered. For example, if the effective confinement thickness is 150 mm, a 450 mm thick base layer could include two geogrids, one at its bottom and the other one 150 mm below the top of the layer (see Slide A.85). The effective confinement thickness is further discussed in Section 5.6.5.

There are fundamental differences between the reinforcement function and the stabilization function in roads:

- Contrary to the reinforcement function, which mostly improves the pavement system, the stabilization function improves the associated material by forming a composite material.
- While tensile forces are transferred to the anchored parts of the geosynthetic in the case where the reinforcement function is performed at the pavement system scale, the stabilization function is effective over the entire area where a geosynthetic/soil composite material is created as a result of close interaction between geosynthetic and soil. The omnipresent nature of the soil-geosynthetic interaction is an essential characteristic of the stabilization function: it is the necessary condition for the formation of a soil-geosynthetic composite material.
- Confinement (which characterizes the stabilization function) is mobilized at low geosynthetic strain when traffic loading is applied. Therefore, stabilization requires only small deformation of the pavement system whereas transferring tensile forces from one part of a system to another one (which characterizes the reinforcement function when it is performed at the scale of the pavement system) may require relatively large deformation of the pavement system – for example significant rutting as in the case of the tensioned membrane effect.
- Since the stabilization function is mobilized at low strain, progressive accumulation of permanent deformation of the soil-geosynthetic composite material under traffic loading is significantly less than in the case of non-stabilized soil. Therefore, base stabilization increases the service life of a road.
- Since the tensioned membrane effect (a mechanism based on the reinforcement function) requires rutting, the traffic must be channelized to mobilize the tensioned membrane effect (see Slides A.127 to A. 141 and A.190 to A.195). In contrast, wandering traffic is not detrimental to the effectiveness of the stabilization function.

The stabilization function is beneficial to both unpaved and paved roads through the mechanisms described in Sections 2.2 and 2.3. The stabilization function is often referred to as 'mechanical stabilization function'. This is because, in most road applications, the stabilization function is the main mode of mechanical improvement of the road. This is further discussed in Section 2.1.4.

Stress-relief interlayer function

A geotextile (generally impregnated with bitumen), used between an original surface course of a paved road and an asphalt overlay, performs the stress-relief interlayer function to minimize stress concentration at the bottom of the overlay, thereby preventing or delaying the formation of cracks induced into the overlay by the repeated movements (due to traffic loading as well as expansion-contraction caused by moisture and/or temperature variations) of cracks in the original surface course (see Slides A.348 to A.370).

There is some similarity between the stress-relief interlayer function and the well-known cushion function performed by geotextiles used to protect geomembranes from concentrated stresses applied by adjacent materials (e.g. puncturing by stones) or construction activities: with both functions, the geotextile reduces concentrated stresses. However, the concentrated stresses related to the two functions are different: in the case of a stress-relief interlayer, the concentrated stresses are tensile stresses parallel to the plane of the geotextile; whereas, in the case of a cushion, the concentrated stresses are normal to the plane of the geotextile or are inclined. Another difference is that, in the case of a stress-relief interlayer, loading is repeated many times, whereas, in the case of a cushion, loading repetition may vary significantly depending on the application. Geotextile cushions are rarely used in roads; two potential applications are presented in Slides A.212 and A.401.

Separation function

A geosynthetic (generally a geotextile) performs the separation function when it prevents intermixing of two materials, with different particle size distributions, that are squeezed together by applied loads, in particular repeated loads.

In roads, the geotextile separator is generally between the subgrade (which often contains fine particles, called 'fines') and the overlying granular material, for example an aggregate base (see Slides A.231 to A.257). Two modes of action are involved in the separation function: (1) prevention of aggregate loss into the subgrade; and (2) prevention of migration into the aggregate pore space of fine particles from the subgrade, a phenomenon caused by repeated traffic loading and referred to as pumping. A properly selected geotextile performs both modes of action, prevention of aggregate loss and prevention of migration of fines into the aggregate layer. In contrast, a geogrid can prevent aggregate loss, but cannot prevent the migration of fines into the aggregate pore space. If a geogrid is used between base and subgrade without a geotextile separator, the particle size distribution of the base material should be such that the filter criteria between the subgrade and the base material are met. (See the discussion of the filtration function hereafter.)

As a result of separation, the integrity of the road is maintained. In particular, the effective thickness of the

base remains as constructed and its modulus is not decreased by the presence of fines that have migrated from the subgrade. Therefore, separation ensures that as-constructed aggregate layer thicknesses and properties are preserved, thereby maintaining the performance of a road and increasing its service life.

Fluid barrier function

A watertight or a low-permeability geosynthetic performs the fluid barrier function when it forms a barrier that prevents or minimizes the migration of fluids (liquid or gas) thereby allowing the containment and the conveyance of fluids. In a paved road, a geotextile impregnated with bitumen, used between an original surface course and an asphalt overlay, performs the fluid barrier function (see Slides A.361 to A.368), thereby preventing precipitation water from infiltrating into the road structure. The same function could be conceivably performed by a geomembrane – that is a geomembrane inserted in a road structure to prevent water infiltration. The fluid-barrier function is also performed by a geomembrane used to construct a road base with the 'membrane-encapsulated soil layer' technique (see Slides A.209 to A.219), and by geomembranes associated with roads built on expansive soil to prevent infiltration of water that would cause the subgrade soil to swell (see Slides A.396 to A.402).

Drainage function

A geosynthetic performs the drainage function when it conveys, within its planar structure, a fluid driven by hydraulic gradient or by capillarity. The drainage function is performed by: (1) a thick nonwoven geotextile, a thick geosynthetic such as a geonet having high hydraulic transmissivity, or a geocomposite (with a high transmissivity core) where water flow is driven by hydraulic gradient, which includes drainage by gravity (see Slides A.196 to A.201); or (2) a wicking geotextile where water migration is driven by capillary suction (see Slides A.201 to A.208). In a road, these geosynthetics are used to evacuate laterally water from various sources: precipitation, runoff from roadside shoulders or slopes, lateral infiltration, capillary rise from the subgrade soil, and so on. Regarding wicking geotextiles, it is important to note that there is no capillary suction in a wicking geotextile when both wicking fibers and surrounding soil are saturated with water; however, a saturated wicking geotextile can still perform the drainage function because it can convey water driven by hydraulic gradient (see Section 3.4.1).

A capillary barrier is a horizontal layer used in a road structure to stop the migration of water by capillarity. Conceptually, a watertight geosynthetic (such as a geomembrane) performing the fluid barrier function could be used as a capillary barrier. However, a different approach is generally used: capillary barriers typically consist of a drainage layer (gravel layer or geosynthetic) in which the pores are sufficiently large so that the potential capillary rise in this drainage layer is less than its thickness. Thus, thick geonets and other innovative geosynthetics can be used as capillary barrier. In a road, water driven by capillarity and migrating upward through the subgrade soil cannot migrate across such a barrier: instead it is re-directed toward the roadside (see Slides A.202 to A.208).

A capillary barrier can also be achieved using a wicking geotextile. The way a wicking geotextile works is opposite to the functioning of a coarse drainage material described above. Whereas a coarse drainage material is the locus of zero capillarity, a wicking geotextile is the locus of high capillarity. Thus, water can be drained toward the sides of the road by a horizontal wicking geotextile. Therefore, a wicking geotextile can act as a capillary barrier by redirecting laterally (thanks to capillarity that takes place within the geotextile) water that tends to rise by capillarity in the soil. Thanks to the suction associated with a wicking geotextile, even water held by capillarity above the wicking geotextile can be drained laterally: the high suction exerted by the wicking geotextile draws, toward the wicking geotextile, water present in adjacent soil located above and below the wicking geotextile.

Filtration function

A geotextile performs the filtration function when it allows water to pass while retaining the soil through which water is flowing. An important benefit of the filtration function is to ensure soil retention without excess water pressure buildup. An essential condition for the long-term performance of filtration is that the particle size distribution of the soil to be retained should be such that a large amount of fine particles do not move within the matrix formed by coarser particles; such soil is called an 'internally stable soil'. If the soil is not internally stable, the following two situations may occur: if the filter openings are small, particles accumulate on the filter and clogging is inevitable; and, if the filter openings are large, internal erosion of the soil takes place. No adequate filter opening size is possible in the majority of cases of non-internally stable soil. In contrast, filter criteria make it possible to select an adequate filter opening size if the soil is internally stable.

In a road, the filtration function is performed by a geotextile that is part of a drainage geocomposite or by a geotextile placed between a drainage layer and the soil. Also, a geotextile used as a separator performs the filtration function, in addition to the separation function, if water percolates in the upward direction from a saturated subgrade through the geotextile and into the overlying material (i.e. the base or the subbase material).

In addition to the usual situation where a filter is retaining an internally stable soil as described above, there is a special situation where a filter is used to stop particles that are carried by water. In this case, the purpose of the filter is to control internal erosion of the soil that tends to develop progressively as soil particles are carried away by water. In this case, particles accumulate on and/or in the filter and, consequently, water pressure buildup may occur. This situation is classical in embankment dams (Giroud 2010) and it may exist under the joints of concrete surface courses where repeated movements of the concrete slabs subjected to traffic loading, associated with the

presence of water in the soil, generate high water pressure and an upward displacement of soil particles. This mechanism, called pumping, causes progressive internal erosion of the soil, resulting in pavement distress due to lack of support of the surface course. Geotextile filters can be used to control this mode of deterioration of paved roads with concrete surface course.

2.1.3. *Groups of functions and means of road improvement*

Groups of functions

As shown in Table 1, the functions presented above can be arranged in groups of functions. The groups of functions correspond to different means of road improvement: mechanical, physical or hydraulic. As seen in Table 1, these three groups of geosynthetic functions can be put in parallel to non-geosynthetic means of improvement: road improvement by chemical means and road improvement by biological means. These different means of road improvement are briefly discussed below.

Road improvement by mechanical means

As indicated in Table 1, 'road improvement by mechanical means' results from the implementation of three functions: reinforcement, stabilization and stress-relief interlayer. The stress-relief interlayer function is related to a special mechanism: the prevention of cracking of asphalt overlays. Therefore, the two main functions that ensure the improvement of a road structure by mechanical means are the reinforcement function and the stabilization function. Many discussions in this paper are devoted to these two functions.

Road improvement by physical means

The well-known function of separation (see Section 2.1.2 above, and Slides A.232 to A.257) maintains the strength and modulus of the base course through two mechanisms, by preventing or delaying: (1) the progressive loss of base course aggregate into the subgrade; and (2) the progressive migration of fines from the subgrade into the base course. As a result, geotextiles, through the separation function, contribute to the long-term performance by preventing or delaying the progressive deterioration of the road structure, thereby maintaining the integrity, modulus and strength of the base course and increasing the service life of unpaved and paved roads. The separation function can be considered a physical means of road improvement, as compaction is a physical means of soil improvement through particle rearrangement (Table 1).

Road improvement by hydraulic means

It is well known that the presence of water in the road structure is detrimental to performance, for example: by reducing the modulus and strength of the base course, by weakening the subgrade soil, by fostering freeze-thaw problems, and so on. Therefore, an important role is played by the following functions: (1) fluid barrier provided by geomembranes or by geotextiles impregnated with bitumen; and (2) drainage provided, for example, by geonets, drainage geocomposites and wicking geotextiles. In many cases, the filtration function performed by a geotextile contributes to the effectiveness of drainage by promoting soil retention without water pressure buildup. These three functions, fluid barrier, drainage and

Table 1. Means, purposes, functions and examples of road improvement using geosynthetics

Means of improvement	Purpose of the group of functions	Function	Examples of road improvement
Mechanical	Reduction of the pavement system deformation	Reinforcement	• Asphalt course reinforcement to minimize rutting and cracking • Load carrying by tensioned membrane effect at high geosynthetic strain • Bearing capacity increase through subgrade heave restraint
		Stabilization (*)	• Lateral restraint due to confinement of base and/or subbase, at low geosynthetic strain, resulting in formation in base and/or subbase of a composite material with high modulus and long-term integrity • Bearing capacity increase as a result of modified stresses on subgrade
		Stress relief interlayer	• Prevention of asphalt overlay cracking by minimizing stress concentration at bottom of overlay
Physical	Prevention of deterioration of the pavement system	Separation	• Prevention of aggregate loss • Prevention of fines migration • Prevention of intermixing of adjacent materials
Hydraulic	Water control in the pavement system	Fluid barrier	• Prevention of water migration into road structure
		Drainage	• Water removal driven by hydraulic gradient: drainage by transmissivity • Water removal driven by capillarity: drainage by wicking
		Filtration	• Soil retention without water pressure buildup
Chemical	Chemical improvement, generally known as 'chemical stabilization', is a well-established method for improving roads, but this method does not involve geosynthetics.		
Biological	Biological improvement methods are currently subjected to intensive research. It is expected that some geotechnical systems, including roads, will benefit from these methods in the future.		

(*) Note: The term 'mechanical stabilization' is sometimes used to designate the stabilization function.

filtration, can be grouped under the category of hydraulic means of road improvement (Table 1).

Road improvement by chemical and biological means
Beyond the field of geosynthetics, chemical means and biological means of road improvement are included in Table 1. The technique known as 'chemical stabilization' (e.g. by lime or cement) is a well-established method for improving roads. Also, it may be predicted that soil improvement by biological means (e.g. by a controlled use of biological material, such as enzymes, bacteria or roots) may become available for road applications in the future as a result of on-going research.

2.1.4 *Uses of the term 'stabilization'*
It is now generally accepted that the term 'stabilization' designates a geosynthetic function (which is related to confinement and stiffening, as indicated in Section 2.1.2). However, phrases such as 'road stabilization by geosynthetics' and 'geosynthetic-stabilized roads' are frequently used. Therefore, the use of the term stabilization needs to be explained.

Since the early 1970s, geotextiles have been extensively used for separation in both paved and unpaved roads, and they have been used for the mechanical improvement of unpaved roads by performing the reinforcement function, in particular through the tensioned membrane effect. With the advent of geogrids in the early 1980s and their successful use for several decades, the stabilization function has become the dominant function to ensure the mechanical improvement of roads. It can be expected that this trend will be confirmed by the growing use of geocells in roads.

As a result of the dominant role of the stabilization function, the phrase 'mechanical stabilization of roads' tends to become synonymous with 'road improvement by mechanical means'; similarly, the term 'road stabilization' tends to become synonymous of 'road improvement by mechanical means' or even 'road improvement by all means'. Furthermore, the stabilization function is often called 'mechanical stabilization'. Discussions presented in this paper may occasionally follow this trend.

2.2. Unpaved road improvement

2.2.1. *Overview of unpaved road improvement*
Geosynthetics may have beneficial effects in unpaved roads through the functions of separation, filtration, drainage and fluid barrier described above in Section 2.1.2. However, only the mechanical means of unpaved road improvement are addressed in this section. There are two essential mechanisms in the mechanical behavior of an unpaved road: load distribution by the base course, and load bearing by the subgrade. Furthermore, in some cases in unpaved roads with significant rutting, part of the wheel load is supported by the geosynthetic tension, which results in load redistribution with reduction of the maximum stress on the subgrade soil. These mechanisms are discussed below.

2.2.2. *Improved load distribution*
In an unpaved road, the base course distributes the load. As a result, the maximum normal stress at the bottom of the base (i.e. on top of the subgrade) is lower than the normal stress at the contact between the wheel and the top of the base course. This is illustrated in Figure 4.

As a result of confinement of the base material, which is the mechanism associated with the stabilization function performed by a geosynthetic, the base course modulus is increased (as explained in Section 2.1.2). This increase of base course modulus results in an increase of the load distribution capacity of the base course. In other words, thanks to stabilization of the base course material provided by the geosynthetic, the maximum stress at the bottom of the base course is lower than in the case without geosynthetic, which improves the road performance. It should be noted that the total load on the subgrade is not reduced by stabilization: the load is better distributed (or 'redistributed') with a lower maximum stress, as illustrated in Slides A.42 to A.48.

The application of a vertical traffic load mobilizes the confinement with limited geosynthetic strain – that is with limited disturbance of the base material. As a result, the rate of base degradation with repeated traffic loading is reduced. Consequently, thanks to base material stabilization by the geosynthetic, the base modulus decreases at a lower rate compared to the rate of modulus decrease in the case without geosynthetic. As a result, the service life of the road is increased.

2.2.3. *Increased subgrade bearing capacity*
The bearing capacity of the subgrade is increased by a geosynthetic performing the reinforcement function through the restraint of subgrade heave. In this case, the geosynthetic transfers tensile forces from between the wheels to the zone where the geosynthetic is anchored. The stresses applied by the geosynthetic to restrain subgrade heave act as a surcharge that increases the subgrade bearing capacity in accordance with the classical

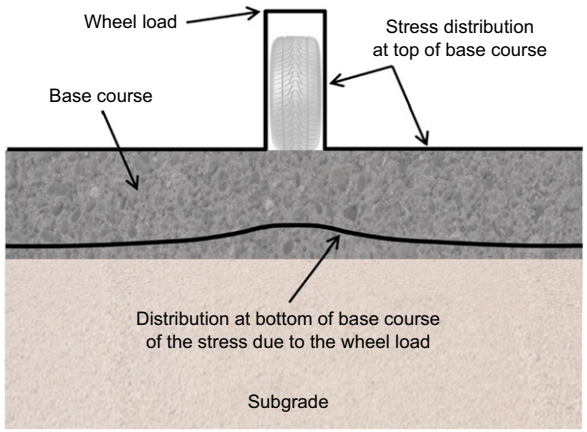

Figure 4. Load distribution by the base course: the maximum stress at the bottom of the base course is much lower than the maximum stress at the top of the base course (i.e. the wheel load). Note: The stress due to the weight of the base course is not considered in the above figure.

bearing capacity theory (see Slides A.142 to A.187, Slides A.272 and A.273, and Slides A.425 to A.430).

The increase in subgrade bearing capacity depends on the inclination of the stresses that constitute the above-mentioned surcharge. According to a classical result of the theory of plasticity, inclined stresses with the shear component oriented toward the load (i.e. 'inward inclined stresses') increase the bearing capacity compared to normal stresses. Two conditions should be met: (1) for the stresses to be inclined, the base/subgrade interface should be rough rather than smooth; and (2) for the stresses to be inclined in the inward direction, the lateral displacement of the base and the geosynthetic should be less than the lateral displacement of the top of the subgrade (in other words, lateral restraint of the base is required). Whether these two conditions are met depends on the type of geosynthetic used to stabilize the base, as discussed below:

- In the case of a geotextile, shear stresses between the geotextile and the subgrade soil are small and can be neglected for the following reasons: interface friction between a woven geotextile and the subgrade soil is low (i.e. rather smooth interface); and a nonwoven geotextile is extensible due to its low modulus (hence limited lateral restraint). In other words, it can be considered that the stresses applied on the subgrade by a geotextile are approximately normal.
- In the case of a geogrid used with an aggregate base, high shear stresses exist between the aggregate base and the subgrade because the following two conditions are met: (i) aggregate that protrudes through the geogrid apertures creates a rough interface with the subgrade; and (ii) thanks to the lateral restraint ensured at low strain by the geogrid, the lateral displacement of the base can be expected to be significantly less than the lateral displacement of the subgrade at the geogrid/subgrade interface. It may, therefore, be concluded that the stresses applied by a geogrid-stabilized aggregate base on the subgrade are inclined inward, with the maximum possible value of the shear stress, which is the undrained shear strength of the subgrade since the subgrade is assumed to be in the saturated undrained case in unpaved road design methods (see Section 3.2.2 and Slide A.143).
- In the case of a geocell, the inclination of the stresses applied on the subgrade depends on the material used to fill the cells and on the presence or not of a geotextile between the geocell and the subgrade. If a geotextile is used (which is often the case), the interface with the subgrade can be considered to be smooth; therefore, in this case, the stresses applied on the subgrade can be considered to be approximately normal.

Thus, based on the bearing capacity factor values for the case of normal stress and the case of inward inclined stresses (see Section 3.3.3) the subgrade bearing capacity increase (compared to the same unpaved road without geosynthetic) is 82%, in the case of a geogrid-stabilized aggregate base, and 64% in the case of a geotextile-stabilized base (see Slides A.180 and A.181).

The above discussion is interesting on two counts: (1) it illustrates that a single geosynthetic can be involved in two mechanisms, lateral restraint of the base course and restraint of the subgrade heave; and (2) it shows that one mechanism (e.g. lateral restraint) due to a certain function (stabilization) may have an impact on the effectiveness of another mechanism (e.g. bearing capacity increase) due to a different function (reinforcement).

The above discussion of the bearing capacity of the subgrade is based on the assumptions that: (1) the subgrade soil is a saturated low-permeability material acting in the undrained mode – that is acting as a frictionless material; and (2) the undrained shear strength, which characterizes this material, is constant over the entire zone of the subgrade soil that is involved in the bearing capacity mechanism (see Slide A.143). If the above assumptions are not met (i.e. if the subgrade soil exhibits friction or the undrained shear strength increases with depth), then the bearing capacity may increase as explained in Slides A.184 to A.187.

2.2.4. *Load redistribution by the tensioned membrane effect*

The tensioned membrane effect (which is described in Slides A.127 to A.141) can be summarized as follows: (1) in an unpaved road, a geosynthetic is located between the base and the subgrade; (2) the geosynthetic deformation is consistent with the deformations of the base and the subgrade associated with rutting; (3) as a result, the portion of geosynthetic under the wheels exhibits a concave shape and is under tension; and (4) consequently, the resultant of the geosynthetic tensions under a wheel is oriented upward and a fraction of the wheel load is thus carried by the geosynthetic. The geosynthetic function, in the tensioned membrane effect, is the reinforcement function since the geosynthetic, which is under tension because it is deformed with a curved shape (i.e. 'out-of-plane deformation'), transfers the tension to the location where it is safely anchored (anchorage being an essential characteristic of the reinforcement function, as mentioned in Section 2.1.2 above). In this case, the relationship between the geosynthetic function (reinforcement) and the mechanism (tensioned membrane effect) appears clearly.

The tensioned membrane effect reduces the maximum load transmitted to the subgrade in unpaved roads (which is a way to contribute to load distribution). However, this mechanism becomes important only in the case of deep rutting (see Slides A.133 to A.136).

It should be noted that the geosynthetic located between the base course and the subgrade performs two functions: (1) it provides stabilization to the base course material by creating a composite material; and (2) in the case of deep rutting, it also provides reinforcement to the unpaved road system by transferring tensile forces through the tensioned membrane effect. This illustrates the fact that, as pointed out in Section 2.1.2, the stabilization

function improves the material, whereas the reinforcement function improves the system.

2.3. Paved road improvement

2.3.1. *Overview of paved road improvement*

Geosynthetics may have beneficial effects in paved roads through the functions of separation, filtration, drainage and fluid barrier described above in Section 2.1.2. However, only the mechanical means of paved road improvement are addressed in this section: the improvement of the structural performance of paved roads and the improvement of asphalt surface courses and asphalt overlays.

2.3.2. *Improvement of the structural performance of paved roads*

The dominant role of the stabilization function in paved roads

There is a difference between unpaved roads and paved roads regarding the mechanisms of road improvement. Among the mechanisms involving geosynthetics that improve the performance or the service life of an unpaved road from a mechanical standpoint, only the lateral restraint of the base material and the resulting load distribution improvement play a significant role in the improved performance and/or increased service life of a paved road. Both mechanisms are related to the same function, the stabilization function (see Section 2.1.2 above and Slide A.299).

The limited role of the reinforcement function in paved roads

In unpaved roads, geosynthetics perform the reinforcement function through two mechanisms: partial load carrying through the tensioned membrane effect; and increase in subgrade bearing capacity through subgrade heave restraint. This is not the case in paved roads, as discussed below.

The load redistribution due to the tensioned membrane effect is negligible in paved roads because rutting is then too small to mobilize this mechanism.

The subgrade bearing capacity improvement, which plays a key role in the improvement of unpaved roads, generally does not play a significant role in paved roads because the stresses on the subgrade (resulting from the distribution of stresses applied by wheel loads) are much lower than in the case of unpaved roads. This is due to the fact that the surface course, the base course and the subbase course of a paved road, working together, distribute the wheel load more effectively than the base course of an unpaved road. Therefore, adding a geosynthetic on top of the subgrade may not effectively reinforce a paved road (even though geosynthetics may have beneficial effects through the functions of separation, filtration, drainage and fluid barrier). As a result, the usual design methods for paved roads do not consider bearing capacity. However, in the case of very soft subgrade, it may be necessary to improve the subgrade bearing capacity for construction purposes. To provide support during construction, a 'capping layer' (also called 'subgrade improvement layer' or 'construction platform') may be placed on top of the soft subgrade, and a geosynthetic may be incorporated into this capping layer to improve it or reduce its thickness.

The above discussion shows that the use of geosynthetics performing the reinforcement function does not provide significant benefits to the structural performance of paved roads. However, geogrids can provide beneficial reinforcement to asphalt layers: asphalt surface courses and asphalt overlays (see Section 2.3.3 hereafter).

Approach to design methods for paved roads

Based on the foregoing discussion of relevant mechanisms, the design methods for paved roads incorporating geosynthetics are focused on the structural improvements that geosynthetic stabilization provides to the pavement layers. The state of practice consists in using the traditional empirical methods, such as the AASHTO (1993) method, with factors that account for the beneficial effect of geosynthetics on the associated layers (see Slides A.300 to A.305). At the same time, mechanistic-empirical design methods that account for the beneficial effect of geosynthetics are being developed (see Section 4.3.3 and Slides A.306 to A.313).

2.3.3 *Improvement of asphalt surface courses and asphalt overlays*

Asphalt surface course reinforcement

In the case of paved roads with asphalt surface course, a geogrid can be used to reinforce the asphalt surface course. This reinforcement reduces the risk of fatigue cracks in the asphalt surface course, and it may reduce the development of rutting within the asphalt surface course (see Slides A.330 to A.332).

Progressive distress of asphalt overlays

When the original asphalt surface course of a road has reached its serviceability limit, rather than replacing it, a layer of asphalt concrete, called 'asphalt overlay', can be placed on this original surface course. If the original asphalt surface course is cracked, the two sides of each crack undergo relative movement as a result of expansion-contraction due to temperature and moisture variations and as a result of repeated traffic loading. The relative movements of the two sides of cracks in the original surface course induce concentrated stresses at the bottom of the overlay. As a result of these concentrated stresses, cracks appear at the bottom of the overlay on top of the cracks of the original surface course. These cracks grow progressively from the bottom to the top of the overlay. As a result, the pattern of cracks in the overlay reflects the pattern of cracks in the original surface course, hence the term 'reflective cracking' (see Slides A.333 to A.345).

Use of geosynthetics in asphalt overlays

Using geogrid reinforcement at the bottom of an asphalt overlay has the following beneficial effects: (1) reduction of the risk of fatigue cracks and, possibly, reduction of rutting within the asphalt overlay, and (2) reduction of the risk of reflective cracking in the asphalt overlay (see Slides A.346 and A.347).

Alternatively, if a nonwoven geotextile impregnated with bitumen is placed between the original asphalt surface course and the asphalt overlay, movements of the edges of cracks deform the nonwoven geotextile impregnated with bitumen (see Slides A.348 to A.360). Thanks to the visco-elastic behavior of the nonwoven geotextile impregnated with bitumen, movements of cracks in the original surface course induce only limited stresses in the asphalt overlay. Therefore, if a nonwoven geotextile impregnated with bitumen, or a geocomposite with similar structure and properties, is placed between the original asphalt surface course and the asphalt overlay, crack development in the asphalt overlay is prevented or delayed. Here, the nonwoven geotextile impregnated with bitumen and the geocomposite perform the stress-relief interlayer function. In addition, the geotextile impregnated with bitumen, and the geocomposite if it is waterproof, perform the fluid barrier function, thereby preventing water from penetrating into the road structure.

In conclusion, two different approaches, involving two different geosynthetic functions, are used to address the reflective cracking issue: geogrid performing the reinforcement function and geotextile impregnated with bitumen performing the stress-relief interlayer function.

3. DESIGN OF GEOSYNTHETIC-IMPROVED UNPAVED ROADS

3.1. Overview

3.1.1. *Unpaved roads and areas*

Unpaved roads have mostly been used as local roads especially in rural areas or as temporary or haul roads in construction sites as shown in Slide B.4. There are unpaved areas that are similar to unpaved roads but are not roads because they are not subjected to the same traffic conditions. Examples include: (1) unpaved shoulders along highway pavements; (2) temporary construction platforms to support construction equipment (e.g. cranes); and (3) unpaved parking lots for limited uses.

Local roads and haul roads are subjected to repeated channelized traffic loading while unpaved shoulders, construction platforms and parking lots are often subjected to stationary loads or non-channelized traffic of low-speed vehicles. This Section 3 of the paper is focused on the design of unpaved roads under repeated traffic loading, assuming that the traffic is channelized.

3.1.2. *Basic concept*

Pavement layers including surface, base, and subbase play important roles in distributing traffic loads to a wide area on the subgrade so that the stresses on the subgrade are low. The use of a pavement surface (concrete or asphalt layer) reduces the stresses significantly enough to avoid bearing failure of the subgrade; as a result, subgrade bearing failure is not a dominant failure mode for paved roads. Instead, deformations (e.g. rutting due to compression of each layer and fatigue failure due to tensile strain at the bottom of the asphalt layer) are the controlling failure modes for asphalt paved road design. On the other hand, without a concrete or asphalt surface layer, the distributed stresses on the subgrade may be high enough to cause bearing failure during the service life. Therefore, rutting due to subgrade bearing failure is often considered for unpaved road design. These concepts are illustrated in Slides B.5 to B.7.

3.1.3. *Needs for geosynthetics*

Strengths of subgrade and aggregate base are often quantified using the California Bearing Ratio (CBR) in roadway design. The detailed procedure for CBR testing is included in ASTM D1883 – 16, which is illustrated in Slide B.8. The undrained shear strength of saturated fine-grained subgrade is often correlated with its CBR value as follows (Slide B.9):

$$c_u = \rho \cdot \mathrm{CBR} \tag{2}$$

where c_u, is the undrained shear strength of subgrade (kPa); CBR is the California Bearing Ratio (%, use the percentage value); and ρ is a factor. The factor ρ typically ranges from 20 to 30. For example, $\rho = 30$ for saturated clays and silty clays, while for sandy clay, clayey sand or silt, ρ has a lower value. The c_u – CBR correlation should be specifically established for critical applications.

Berg *et al.* (2000) (Slide B.10) suggested that a nonwoven geotextile may be used as a separator if a soaked subgrade CBR is higher than 3%; a geogrid or woven geotextile may be used as a reinforcement if the soaked subgrade CBR is higher than 1% but lower than 3%; and a geogrid associated with a nonwoven geotextile or woven geotextile may be used as a separator as well as a reinforcement if the soaked subgrade CBR is lower than 1%.

McGown and Ozelton (1973) described the loss of base material by penetration into the subgrade and the migration of fines from the subgrade into the base or subbase. Leflaive and Puig (1973) dealt with interpenetration of two soil layers and the action of a 'textile' to prevent the mixing of these two layers. Based on field observations, Christopher and Holtz (1989) found that, without a geosynthetic separator, aggregate base material would be lost during its service due to inter-mixing of aggregate and soft subgrade soil, as shown in Slide B.11. This aggregate loss reduces the thickness of the base course. The subgrade with a lower CBR has a higher percentage of aggregate loss. When nonwoven or woven geotextile is used, it can prevent aggregate from being pushed into soft subgrade and it can minimize migration of fine particles from subgrade into aggregate (Slide B.12). Therefore, aggregate loss can be prevented or minimized. Filtration design is required to ensure the effectiveness of the geotextile. When a geogrid (without geotextile) is used between aggregate base and subgrade, it may maintain the integrity of the aggregate base by interlocking with the aggregate particles, thereby restricting aggregate displacement and preventing aggregate particles from being pushed into soft subgrade (Slide B.13). The effectiveness of the geogrid in minimizing aggregate loss also depends on filtration requirements between aggregate

and subgrade. As pointed out by Anderson (2006), if there is no geotextile separator, the aggregate base material should meet the filtration requirements as presented in Slide B.14 to minimize migration of fine particles from the subgrade into the base.

To effectively perform their functions, geosynthetics should survive during construction. AASHTO (1990) provides a guide for selecting: (1) the minimum compacted base thickness (at least 100 mm); and (2) the class of geotextile based on site subgrade CBR (ranging from lower than 1% to higher than 3%) and equipment ground contact pressure (lower or higher than 350 kPa). Holtz *et al*. (2008) provides a similar guide for cases where a geogrid is used. These guides suggest that a higher class of geotextile or geogrid be used for a lower subgrade CBR and/or a higher equipment ground contact pressure.

3.2. Two early design methods for unpaved roads

3.2.1. *The Steward* et al. *method*

The Steward *et al*. method (Steward *et al*. 1977) (Slide B.16) was based on the modification of the method developed by Barenberg *et al*. (1975) for a specific geotextile. In this method, the Boussinesq solution was used for determining the maximum vertical stress on top of the subgrade under a circular load applied at the ground surface. The calculated maximum vertical stress should be lower than the bearing capacity of the subgrade, which is defined as

$$p_i < q_u (= N_c c_u) \tag{3}$$

where p_i is the maximum vertical stress on top of the subgrade calculated using the Boussinesq solution for a homogeneous half-space; q_u is the bearing capacity of subgrade soil; and N_c is the bearing capacity factor.

Steward *et al*. (1977) proposed different bearing capacity factors for unpaved roads without geotextile and with geotextile depending on the rutting depth and the number of passes of a standard axle (80 kN) as shown in Slide B.16. The bearing capacity factors for the roads without geotextile range from 2.8 to 3.3 while the factors with geotextile are 5.0 to 6.0. The design concept and steps for this method are presented in Slides B.17 and B.18. To help engineers to use this method for actual design, Steward *et al*. (1977) developed several design charts included in the US Federal Highway Administration (FHWA) document – Geosynthetic Design and Construction Guidelines (FHWA HI-95-038) (Holtz *et al*. 1998). Two of these design charts are shown in Slides B.19 and B.20. The limitations of this method include (Slide B.21): (1) load distribution is determined without taking into account base material properties; (2) influence of rut depth and number of passes are considered approximately and are limited to two cases; (3) there is no theoretical background for the bearing capacity factors; (4) tensioned membrane effect is not included; (5) this method is only limited to geotextiles; and (6) geotextile properties are not specified.

3.2.2. *The Giroud and Noiray method*

Giroud and Noiray (1981) developed a design method that provides a quantification of the tensioned membrane effect and considers stress distribution and the increased bearing capacity factor due to the subgrade heave restraint by the geotextile as an additional surcharge. The Giroud and Noiray method quantifies the effect of the reinforcement function of geotextiles in unpaved roads, hence the use of the terms 'reinforced' and 'unreinforced' below. This method includes four steps (Slides B.22 to B.28): (1) determine the required base thickness for an unreinforced case under traffic in terms of passes using the simplified U.S. Army Corps method (h), (2) determine the required base thickness for the unreinforced and reinforced cases under a static load (h_0 and h_r), (3) determine the reduction of base thickness ($\Delta h = h_0 - h_r$) under a static load, and (4) determine the required base thickness for the reinforced case ($h' = h - \Delta h$) under traffic loading by applying the base thickness reduction to the required base thickness determined in Step 1. Giroud and Noiray (1981) assumed that a wheel load is distributed from the base to the subgrade at a distribution angle of 31° (i.e. $\tan\alpha = 0.6$). They suggested that the distributed vertical stress on the subgrade in an unreinforced road should be limited to the elastic limit (i.e. $\pi c_u = 3.14 c_u$) to avoid excessive deformation. However, in a geotextile-reinforced road, the distributed vertical stress on the subgrade is allowed to be as high as the plastic limit (i.e. $(\pi + 2)c_u = 5.14 c_u$) due to the subgrade heave restraint by the geotextile providing an additional surcharge. In addition, the vertical component of the tensile force in the geotextile due to the tensioned membrane effect reduces the vertical stress on the subgrade.

The approach described above leads to the following equation, which can be used to calculate the required base thicknesses for unreinforced and geotextile-reinforced sections:

$$\frac{P_a}{2(B + 2h\tan\alpha)(L + 2h\tan\alpha)} - \frac{J_g \varepsilon_g}{a\left(1 + (0.5a/s_e)^2\right)^{0.5}} = N_c c_u \tag{4}$$

where P_a is the axle load; B and L are the width and length of a tire contact area, respectively; h is the base thickness; a is the half length of the chord of the deflected geotextile; s_e is the elevation rut depth (i.e. the vertical distance between the initial elevation of the road surface and the elevation of the rut bottom) at the interface between base and subgrade; α is the stress distribution angle from the base to the subgrade; J_g is the geotextile tensile stiffness (0 for an unreinforced section; no creep or relaxation is considered) determined by a wide-width strip method (ASTM D4595); ε_g is the geotextile tensile strain; c_u is the undrained shear strength of the subgrade; and N_c is the bearing capacity factor (3.14 for an unreinforced section and 5.14 for a geotextile-reinforced section) (Slide B.27). It should be noted that, in the Giroud and Noiray method, the elevation rut depth is used to calculate the reduced vertical stress on subgrade due to the geosynthetic,

whereas the apparent rut depth is used to correct the number of axle load passes (the apparent rut depth being defined as the vertical distance between the highest point of the deformed road surface and the rut bottom, sometimes defined as the vertical distance between peak and valley of the deformed road surface).

Based on calculations done with the Giroud and Noiray method (Slides B.29 and B.30), the tensioned membrane effect is negligible for apparent rut depths of 75 mm or less. It happens that a rut depth of 75 mm is a typical serviceability limit. However, in some cases, unpaved roads can be used with a greater rut depth. For example, Giroud and Noiray (1981) use a rut depth of 300 mm in a design example, which is a very large rut depth. In fact, a maximum rut depth of 150 mm is generally recommended because larger rut depths may result in several problems, such as safety of vehicles, disturbance of roadbed for future construction, and change of the tire contact area (thus changing the tire contact pressure, which may invalidate the design method).

The limitations of the Giroud and Noiray method (Slide B.31) are: (1) no consideration of base material properties, (2) fixed stress distribution angle, (3) base thickness reduction based on static loading rather than cyclic loading, (4) no difference among all geosynthetics, except for the tensioned membrane effect, and (5) influence of axle load magnitude on number of axle passes based on the empirical relationship for paved roads.

It is well known that polymeric materials like geotextiles exhibit creep behavior. Bathurst and Naftchali (2021) demonstrated through a large database that the tensile stiffness of geosynthetics changes with time due to creep and relaxation. Due to the nature of loading and unloading cycles of a traffic load, it is approximate and reasonable not to consider the effect of creep and relaxation on the geotextile tensile stiffness for road applications.

3.3. Design of geosynthetic-stabilized unpaved roads

3.3.1. *Introduction*

The details of the development and verification of the design method generally referred to as the 'Giroud-Han method' are presented in two companion papers published by Giroud and Han (2004a 2004b) (Slide B.33). This method has been included in the FHWA reference manual – Geosynthetic Design and Construction Guidelines (Holtz *et al.* 2008) (Slide B.34). The Giroud-Han method is considered an improved method (Slide B.35) compared to the Giroud and Noiray method (Giroud and Noiray 1981) because of: (1) consideration of base material properties, (2) stress distribution angle varying with traffic passes, (3) base thickness reduction based on cyclic loading, (4) differentiation between geogrid and geotextile and between different geogrids, (5) influence of rut depth based on the subgrade stress-strain relationship, and (6) calibration and verification using field data. A brief description of this method is presented below.

3.3.2. *Base course material requirement*

The base course material should be strong enough to avoid possible failure within the base course under wheel loading (Slide B.36), which is assumed in the Giroud-Han method. Hammitt (1970) developed a design chart as shown on Slide B.37 for an unpaved road, which can be used to check whether a base course material with a certain CBR is strong enough to support a single wheel load for a certain number of passes. If the base course material is not strong enough, a stronger base course material should be used or the base course material should be improved – for example by geogrid or geocell.

3.3.3. *Design against subgrade bearing failure*

Based on the measured vertical stress at the center of the interface between the base course and the subgrade, which increases with the number of load cycles, Giroud and Han (2004b) proposed that the stress distribution angle decreases with the number of load cycles until bearing failure of the subgrade as shown in Slide B.38. The rate of the stress distribution angle reduction depends on the base thickness, the tire contact area, and the properties of geosynthetic if used. This relationship will be discussed later.

Giroud and Han (2004a 2004b) also used the stress distribution method to estimate the vertical stress on top of the subgrade, but assumed a circular tire contact area rather than the rectangular area used in Giroud and Noiray (1981). To prevent bearing failure of the subgrade, the following condition should be met (Slide B.39):

$$p_i = \frac{P}{\pi(r + h\tan\alpha)^2} \leq m\,N_c\,c_u \tag{5}$$

where p_i is the maximum vertical stress on top of the subgrade; P is the wheel load; r is the radius of the tire contact area; h is the base thickness; m is the bearing capacity mobilization factor; N_c is the bearing capacity factor; and c_u is the undrained shear strength of the subgrade.

Giroud and Han (2004a 2004b) used the following values of the bearing capacity factor: 3.14 for non-stabilized unpaved roads and 5.14 for geotextile-stabilized unpaved roads. Considering the rough interface between aggregate-interlocked geogrid and subgrade, Giroud and Han (2004a 2004b) proposed a bearing capacity factor of 5.71 for geogrid-stabilized unpaved roads (Slide B.40).

Giroud and Han (2004a 2004b) recognized that the subgrade resistance is mobilized in relation to the rut depth of the wheel path and proposed a bearing capacity mobilization factor, m, and an empirical equation to account for key influence factors including the rut depth, the radius of the tire contact area, and the base thickness (Slide B.41):

$$m = \left(\frac{s_a}{f_s}\right)\left[1 - \xi\exp\left(-\omega\left(\frac{r}{h}\right)^n\right)\right] \tag{6}$$

where s_a is the apparent rut depth at the surface (defined in Section 3.2.2 as the vertical distance between peak and valley of the deformed road surface); f_s is the serviceability

limit for the apparent rut depth at the surface (typically 75 mm); r is the radius of the tire contact area; h is the base thickness; and ξ, ω, n are constants to be calibrated with field data.

Giroud and Han (2004a) further recognized that the stress distribution from an upper layer to a lower layer depends on the modulus ratio of these two layers and proposed a simplified formula using the theoretical results obtained by Burmister (1958) based on the layered elastic theory (Slide B.42):

$$\tan\alpha_1 = \tan\alpha_0\left[1 + 0.204\left(\frac{E_{bc}}{E_{sg}} - 1\right)\right] \tag{7}$$

where α_1 is the stress distribution angle from the base course to the subgrade under static loading; α_0 is the stress distribution angle for a uniform medium; E_{bc} is the modulus of the base course; and E_{sg} is the modulus of the subgrade.

Based on the measured vertical stresses at the interface of base and subgrade under cyclic plate loading tests in Gabr (2001), Giroud and Han (2004b) back-calculated the stress distribution angle with the number of load cycles and proposed the following empirical relationship (Slide B.43):

$$\frac{1}{\tan\alpha} = \frac{1}{\tan\alpha_1} + \lambda\log N \tag{8}$$

where α is the stress distribution angle at the number of load cycles, N; α_1 is the stress distribution angle at the number of load cycles equal to 1 (i.e. static loading); and λ is the distribution angle reduction rate.

Based on the data analysis, Giroud and Han (2004b) found that the stress distribution angle reduction rate depends on the property of the geogrid and the thickness of the base course, and can be correlated to the aperture stability modulus of the geogrid, J, as shown in Slides B.44 and B.45. The aperture stability modulus of a geogrid, J, can be measured following the ASTM D7864/D7864M - 15 (see Slide B.46 for the test device).

The field data from Hammitt (1970) for non-stabilized unpaved roads were used to calibrate the constants in the above-mentioned equations, thus resulting in the following equation (Slide B.47):

$$h = \frac{\left[0.868 + \left(0.661 - 1.006J^2\right)(r/h)^{1.5}\right]\log N}{1 + 0.204\left(E_{bc}/E_{sg} - 1\right)} \times \left\{\sqrt{\frac{P/(\pi r^2)}{(s_a/f_s)\left[1 - 0.9\exp\left(-(r/h)^2\right)\right]N_c\, c_u}} - 1\right\} r \tag{9}$$

The parameters in the above equation have been defined earlier.

Giroud and Han (2004b) developed two design charts as shown in Slides B.48 and B.49 to help engineers to use their method for actual design.

Additional cyclic plate loading tests conducted by Qian *et al.* (2013a) (see Slide B.50) confirmed the relationship between 1/tanα and the number of load cycles, N, for geogrids with triangular apertures as shown in Slide B.51.

3.3.4. *Design of geocell-stabilized unpaved roads*

The formula for the geotextile and geogrid-stabilized unpaved roads in Equation (9) can be simplified as follows for the case where the geosynthetic is a geocell (Slide B.53):

$$h = \frac{(0.868 + k)\log N}{1 + 0.204\left(E_{bc}/E_{sg} - 1\right)} \times \left\{\sqrt{\frac{P/(\pi r^2)}{(s_a/f_s)\left[1 - 0.9\exp\left(-(r/h)^2\right)\right]N_c\, c_u}} - 1\right\} r \tag{10}$$

The parameter, k, depends on the properties of the geocell, such as cell dimension, material, and manufacturing process; therefore, it should be calibrated for different geocells. Before this calibration, the additional benefit of geocell confinement on the increase of base modulus should be considered. To quantify the base modulus increase due to closed confinement by geocell, a modulus improvement factor (MIF) was proposed by Han *et al.* (2007) as the ratio of the modulus of the geocell-stabilized base to that of the non-stabilized base (Slide B.54). Research shows that the MIF typically ranges from 1.5 to 2.5 for geocell-stabilized aggregate bases. Based on laboratory cyclic plate loading tests and accelerated moving wheel tests on sand, reclaimed asphalt pavement (RAP) aggregate, and well-graded limestone aggregate over weak subgrade, the k parameter was calibrated to be $0.52(r/h)^{1.5}$ (r is the radius of the tire contact area and h is the base thickness) for a specific geocell with a fill cover of 50 to 75 mm (Pokharel 2010) (Slide B.55). The fill cover is an aggregate layer placed above the geocell to protect the geocell from damage by compaction equipment and wheels.

3.4. Recent research on wicking geotextile-improved unpaved roads

3.4.1. *Basic concept of wicking geotextiles*

A wicking geotextile is a woven geotextile in which special fibers are included in the transverse direction. These special fibers, with an average diameter of 30 to 50 μm, have deep grooves (i.e. micro-channels) on their surface with an average groove opening of 5 to 12 μm. The cross-section and micro-structure of these fibers are shown in Slide B.57. Since these micro-channels have large surface areas, they can generate large capillary forces when they interact with water. The capillary forces can suck water from the surrounding soil into the micro-channels and transfer it along these micro-channels out of the soil where it evaporates into air. This process will

continue until the suction in the fibers is equal to that in the soil.

3.4.2. *Functions of wicking geotextiles*

Main function of a wicking geotextile

The main function performed by a wicking geotextile is the drainage function. Thus, wicking geotextiles provide: (1) lateral drainage to stop water capillary rise from fine-grained subgrades, and (2) lateral drainage to remove water from aggregate bases. These two aspects of lateral drainage are discussed below.

The wicking fibers of a wicking geotextile generate suction that may overcome the capillary force in the soil, thereby stopping the upward migration of water from the subgrade to the base. Slide B.59 shows the benefit of a wicking geotextile as a capillary barrier to break the capillary rise at the interface between base and subgrade. Since a wicking geotextile maintains the quality of the base course by providing separation and keeping a constant moisture content in the base course by creating a capillary barrier, the modulus of the base course is maintained.

Wang *et al*. (2017) demonstrated that a wicking geotextile could provide gravitational drainage laterally when the aggregate base was saturated and continue wicking drainage when the aggregate base was unsaturated. Slide B.60 illustrates lateral drainage by a wicking geotextile in a pavement section.

Additional functions of a wicking geotextile

Han *et al*. (2018) have shown that a wicking geotextile, in addition to the drainage function, can perform the following two functions that other geotextiles can perform: (1) the separation function to prevent intermixing of aggregate base and fine-grained subgrade, and (2) the stabilization function by providing lateral restraint through friction between base and subbase.

The lateral restraint of aggregate by the geotextile and the moisture reduction of the aggregate base can increase the modulus of the aggregate base.

3.4.3. *Tests on wicking geotextiles*

Tests demonstrating the functioning of wicking geotextiles

Han and Zhang (2014) reported vertical wicking tests that demonstrate the wicking effect of a wicking geotextile, as shown in Slide B.61. Han *et al*. (2018) also demonstrated the removal of water from a water beaker or jar by a wicking geotextile as compared with a non-wicking geotextile, as shown in Slide B.62.

Guo *et al*. (2019) reported that a wicking geotextile was effective to reduce the moisture content in an aggregate base within a certain distance (approximately 200 mm for the aggregate with 10% fines used in their study) above the geotextile (Slides B.63 and B.64). This study also demonstrated that the wicking geotextile was more effective to reduce the moisture content in the aggregate base than the non-wicking geotextile, especially when the aggregate became unsaturated.

Tests demonstrating the benefits of wicking geotextiles

The field study conducted by Zhang *et al*. (2014) demonstrated the prevention of frost boils in Alaskan roads by removing water in the aggregate base and preventing capillary rise from the subgrade.

Guo (2018) and Han *et al*. (2018) reported large-scale cyclic plate loading tests conducted on unpaved road sections subjected to rainfall to evaluate the beneficial effect of drainage by a wicking geotextile on road performance. Slides B.65 to B.67 show the large test box and the test setup including the test section, the loading plate, the rainfall simulator, and the temperature and relative humidity control. Six tests were conducted with three different stabilization conditions (control, wicking geotextile, and non-wicking geotextile) on two different subgrade CBRs (approximately 3% and 5%). In each test series, three rainfalls were simulated for three different drainage time periods (7 days, 2 days, and 2 h). At the end of each drainage period, 1000 load cycles with a magnitude of 138 kPa were applied and permanent deformations of the load plate were measured. Slide B.68 shows that the use of the non-wicking geotextile reduced the permanent deformation of the test section as compared with the control section. The use of the wicking geotextile further reduced the permanent deformation of the test section as compared with the non-wicking geotextile section.

3.5. Case studies

3.5.1. *Geosynthetic-stabilized unpaved road*

White *et al*. (2010) reported test roads in Weirton, West Virginia, investigating the lateral restraint effect in base course. Slide B.71 shows four test sections on the site, including one control section, one woven geotextile-stabilized section, one biaxial geogrid-stabilized section, and one triaxial geogrid-stabilized section. The properties of the geosynthetics, subgrade, and base are provided in Slide B.72. The specifications of the test truck and the CBR values of the subgrade and the base are provided in Slide B.73. The subgrade CBR value was approximately 3% and the ratio of the base CBR to the subgrade CBR was approximately 15. Slide B.74 shows the preparation of the test section including excavation and leveling of the ground, compaction of the subgrade, placement of the geosynthetic on the subgrade, and placement and compaction of the aggregate base.

In this field study, earth pressure cells were placed vertically in the base and subgrade to measure the horizontal earth pressures and placed horizontally to measure the vertical earth pressure on the top of the geosynthetic (Slide B.75). Slide B.76 shows the measured vertical and horizontal stresses in these test sections. It appears that the vertical stresses in these test sections were similar except for the test section with the biaxial geogrid. The reason for this exception is not clear. More importantly, lower horizontal stresses developed in the subgrade below the geosynthetic while higher horizontal stresses developed in the base above the geosynthetic due to the lateral restraint effect. The geogrid with triangular apertures was more effective than the other geosynthetics.

White *et al.* (2010) evaluated the performance of the geosynthetic by proposing a 'reinforcement ratio' as shown in Slide B.77, which is defined as the ratio of the lateral earth pressure coefficient in the base to that in the subgrade. The term 'reinforcement ratio' is hereafter replaced by 'stabilization ratio' considering the function actually performed by the geosynthetic, as discussed earlier in this paper. The lateral earth pressure coefficient is calculated as the measured horizontal earth pressure divided by the measured vertical earth pressure. A higher stabilization ratio indicates better lateral restraint – therefore, better stabilization. All the test sections with geosynthetics had higher stabilization ratios than the control section and the test section with the triaxial geogrid had the highest stabilization ratio, thus providing the best stabilization.

3.5.2. *Geocell-stabilized unpaved road*

Pokharel (2013, Personal Communication to J. Han on use of geocells to stabilize an access road to a drilling site on the Christina Lake, Alberta, Canada) reported the use of geocells to stabilize an access road to a drilling site, on Christina Lake in Alberta, Canada, which consisted of a 1.5 m thick muskeg (peat) subgrade (Slide B.79). Slide B.80 shows the weak subgrade before geocell stabilization. The project required the road to support CL-800 truck trailers (i.e. 800 kN as the total semi-trailer load, see Slide B.82 for the dual axles of the truck) for 2.5 million ESALs with a tolerable apparent rut depth of maximum 75 mm. The 2.5 million ESALs were roughly estimated using Equation (1), based on the type of vehicle used on this road.

This geocell-stabilized unpaved road included two layers of geocell in the swamp area (lower layer used as construction platform) and one layer in other areas. The height of geocell was 150 mm and the width of geocell-covered area was 8 m. The fill thickness between geocell layers varied with base thickness, minimum 50 mm and maximum 500 mm. The infill material was a local sand. A 175 mm thick cover, consisting of gravel with particles smaller than 40 mm, was required to avoid damages from grader operation. Slides B.83 to B.90 show the following construction steps: placement of the nonwoven geotextile, deployment of geocells, installation of wooden stakes, anchoring of geocells on the wooden stakes, connection of neighboring geocells by staplers, placement of infill sand, and compaction. Finally, Slide B.91 shows the use of this geocell-stabilized unpaved road for truck traffic.

3.5.3. *Wicking geotextile-improved unpaved road*

Zhang *et al.* (2014) reported the use of a wicking geotextile to mitigate freeze-thaw problems for an access road to oil fields at Beaver Slide on the Dalton Highway, Alaska, USA. The aggregate used for the base course had 6% fines. Due to water infiltration from rainfall, water flowing from side slopes and moisture capillary rise from the fine-grained subgrade, water often accumulated in the aggregate base. As a result of freeze-thaw cycles, frost boils/soft spots were formed on the road and caused excessive rutting under traffic loading. Frequent maintenance and even re-construction of this road were needed. As a field trial, two layers of wicking geotextiles were included in a test section (see Slide B.93) and installed in the field (see Slide B.94). The lower layer of wicking geotextile was placed at the interface between base and subgrade at a depth of 1.2 m from the surface while the upper layer of wicking geotextile was placed within the base at a depth of 0.9 m. The lower layer served as a capillary barrier while the upper layer served as a lateral drainage layer. Moisture and temperature sensors were installed in the test section as shown in Slide B.95. This test section received rainfall on September 6th, 2010 and the volumetric moisture content of the aggregate base became higher than 30% as shown in Slide B.96. Eleven days later (i.e. September 17th, 2010) the moisture contents measured in the aggregate base were much reduced in more than half of the test section. Five days later, the majority of the test section had significant reduction in the moisture content, except for the left corner, which was close to the water source from the side slope and far away from the water exit end of the wicking geotextile. Slide B.96 shows the performance comparison of the same road section before and after improvement by wicking geotextile. Clearly, the wicking geotextile successfully mitigated the freeze-thaw problems of this road.

3.6. Concluding remarks for geosynthetic-improved unpaved roads

The following concluding remarks can be made on the use of geosynthetics for improvement of unpaved roads, and in particular their stabilization:

- Geosynthetics have been successfully used to stabilize soft subgrade and base courses, thus reducing rut depths, reducing required base thickness, and/or prolonging life of unpaved roads.
- Different methods are available to design geosynthetic-stabilized unpaved roads over soft subgrade. They all assume a stable base course and no inter-mixing between base course and subgrade. All design methods have limitations.
- The Giroud-Han design method was developed based on (1) stress distribution concept taking into account a reduced rate of stress distribution angle decrease with traffic thanks to stabilization resulting from aggregate-geogrid interlocking, and (2) bearing capacity theory, taking into account different subgrade bearing capacities for the case of geogrid reinforcement and the case of geotextile reinforcement. The Giroud-Han method is generic, even though it was initially calibrated with two specific biaxial geogrids using laboratory tests and field data reported in the original papers published in 2004. The calibration of the Giroud-Han method has recently been done for one specific geocell-stabilized unpaved road; it considers the benefit of improved base modulus resulting from confinement of base material by this specific geocell. The Giroud-Han method can result in adequate design only if (1) the method is used for geosynthetic products for which it has been

calibrated, (2) the basic assumptions for the method are met, and (3) the method is properly evaluated against reliable field data related to the considered geosynthetic.
- Tests carried out with a wicking geotextile have shown the following: the wicking geotextile could remove water from soil under an unsaturated condition and at optimum moisture content; the wicking geotextile was more effective in reducing water content with time than a non-wicking geotextile; the ability of removing water from soil by the wicking geotextile depended on temperature, relative humidity, and distance to the wicking geotextile; the wicking geotextile significantly reduced permanent deformations of test sections under cyclic loading; the wicking geotextile increased the modulus of base by stabilization (lateral restraint by friction) and drainage (reduction of water content); and the wicking geotextile effectively removed moisture and mitigated freeze-thaw problems.

4. DESIGN OF GEOSYNTHETIC-IMPROVED PAVED ROADS

4.1. Overview

4.1.1. *Types of paved roads*

Pavements are multi-layered structures built on natural or improved subgrade soil to maintain a surface capable of allowing traffic to move in a safe and speedy manner. Paved roads are higher functionality class roads, such as principal and minor arterials (interstates, freeways, etc.) and collectors, that serve most of the traffic whereas they often represent only a small percentage of the road network. Flexible pavements are those with surface layers constructed using asphaltic materials [asphalt concrete (AC) or hot-mix asphalt (HMA)] and often supported by unbound (granular) materials as base and subbase layers. Rigid pavements are those with surface layers made of Portland cement concrete (PCC) slabs and supported by unbound (granular) or asphalt/cement stabilized base and/or subbase layers. Composite pavements can either be constructed as new but often as rehabilitated pavements having both concrete and asphalt materials in the surface layers with either asphalt placed on top of concrete or concrete on top of asphalt. Section 4 of this paper and the related Presentation C are focused on paved roads constructed as highway and airfield pavements, and subjected to repeated loading effects of both vehicular traffic and environment (due to temperature and moisture content changes).

4.1.2. *Basic concept*

Surface layers of paved flexible, rigid and composite pavements are designed to accommodate repeated traffic and environmental loads, provide skid resistance and ride comfort, and resist traffic abrasion. Base and subbase courses support the surface course in a uniform manner, provide a smooth construction platform for the layer above, provide drainage related to surface water infiltration, and prevent pumping caused by wet fine-grained subgrade soils. The subgrade is the lowest and often the weakest layer in a pavement structure, which is compacted and prepared as the roadbed on which pavement layers and shoulders are constructed. Weak subgrades are often improved for load bearing through chemical or mechanical stabilization, or by means of constructing aggregate working platforms. The basic concept of multi-layered pavement structure requires properly distributing wheel loads through the surface, base and subbase courses such that stronger layers are adequately placed on top of weaker layers. Accordingly, the use of a pavement surface (concrete or asphalt layer) and intermediate base and subbase layers significantly reduces the stresses on top of subgrade and protects the pavement foundation. Paved road layer thicknesses are determined through design procedures which define failure of the pavement structure by specifying certain limits for pavement distresses (e.g. permanent deformation or rutting due to compression of each layer and cracking of the surface layer) under the required traffic and environment loads.

4.1.3 *Need for geosynthetics*

Range of applications of geosynthetics in paved roads

Over the past four decades, geosynthetics have been utilized in both bound and unbound layers of pavement structures in a wide range of applications. In unbound layers, geosynthetics have been used (within the unbound material or at the interface between unbound base or subbase layer and subgrade) for separation/filtration, stabilization, drainage, reinforcement and as moisture barrier, as discussed by Koerner (1984) and Holtz *et al*. (1998). In bound wearing courses such as hot-mix asphalt (HMA), geosynthetics have been utilized for tensile reinforcement and as stress-relief interlayers to reduce the potential of reflective cracking (Koerner 1984).

The FHWA publication no. NHI-07-092 summarizes uses of geosynthetics in pavements and roadways, as illustrated in Slides C.5 to C.9, and establishes guidelines for design and construction of pavements with geosynthetics (Holtz *et al*. 2008). The potential geosynthetic applications are mainly illustrated in a multi-layered conventional flexible (asphalt) pavement (see definition in Section 1.2.2). Geotextiles and geogrids, as common geosynthetic types used in road applications, can provide reinforcement in the HMA layer to reduce the permanent deformation in the HMA layer (referred to herein as 'primary rutting'), and reflective cracking. Geotextiles impregnated with bitumen can also serve as a moisture barrier under a cracked pavement surface and on top of subgrade. Geocomposites and nonwoven geotextiles can provide lateral drainage at the interfaces of asphalt and base as well as at the interfaces of subbase and subgrade; and geocomposites installed vertically can be used as edge drains. Geotextiles can prevent subgrade and aggregate base course from inter-mixing, thus maintaining effective

aggregate thickness through separation. Further, geotextiles can act as filters to avoid pumping of soil fines and prevent subgrade water from transporting fines; whereas geogrids are more effective in stabilization/reinforcement applications (see Slides C.7 to C.12).

Location of geosynthetics in pavement structures
Geosynthetics have been typically associated with the unbound layers of pavement structures for the following applications intended to improve the unbound materials performance: (1) under or within an aggregate base or subbase layer typically intended as a lateral restraint to reduce the lateral movement (spreading) of the granular material and locally increase its modulus and strength characteristics, (2) beneath any aggregate base or subbase material as separation/stabilization layers, and (3) beneath, within, or on top of an aggregate base layer as drainage layers; and (4) above or within the subgrade as a capillary break layer. According to FHWA NHI-07-092 (Holtz *et al*. 2008) document (see chart in Slide C.9), subgrade restraint or weak subgrade stabilization application is considered for weak subgrades having California Bearing Ratios (CBRs) less than 3% (Holtz *et al*. 2008). For the most effective uses of geosynthetics for both the separation and base stabilization/reinforcement, subgrade CBR values are indicated to range between 3% and 8% (Holtz *et al*. 2008).

Quantification of the benefits of geosynthetics on pavement performance
An extensive review was conducted on the application of geosynthetics in pavement systems and the related modeling efforts (Al-Qadi *et al*. 2008a). This included a review of the areas of application of geosynthetics, existing pavement design methods that consider geosynthetics, and related specifications and construction practices. These reviews demonstrated the need to quantify the benefit of geosynthetics on pavement performance. Procedures for quantifying the positive contribution of these materials in enhancing pavement performance can be very useful for pavement designers in determining the payoff that could be realized from using the appropriate geosynthetic for specific applications given that proper installation has been achieved. Overall, benefits of geosynthetics in paved roads can be quantified by either reducing structural layer thickness requirements or extending pavement service life for the same pavement layer thicknesses, as illustrated in Slide C.8.

4.2. Geosynthetics for asphalt reinforcement

4.2.1. *Uses of geosynthetics to improve asphalt concrete performance*
Flexible pavements commonly fail through excessive cracking of the asphalt surface or rutting in the wheel path. As illustrated in Slides C.13 to C.15, cracks appearing on the asphalt surface can be caused by load related fatigue, thermal and block cracks due to daily and seasonal temperature changes, cracks occurring due to surface stresses such as shear loading induced by braking vehicles and top down shear cracks, cracks occurring due to lack of support or settlement underneath the HMA layer, and finally, reflective cracks which typically occur in asphalt overlays due to existing joints, cracks or other discontinuities in the original underlying pavement. Geosynthetics have been utilized in flexible pavements for tensile reinforcement to minimize the primary rutting and cracking in HMA surface course and as reinforcement and stress absorption membrane interlayers to reduce the potential of reflective cracking (Koerner 1984). When used as asphalt reinforcement, geosynthetics can increase pavement fatigue life by delaying crack formation, reduce asphalt rutting, and strengthen overlays to reduce reflective cracking. Stiff geogrids are often the preferred type of geosynthetic for asphalt reinforcement. Bitumen-impregnated geotextiles can provide a waterproofing layer below an overlay when cracking does develop.

4.2.2. *Use of geosynthetics to reduce fatigue cracking*
To reduce bottom-up fatigue cracking, geosynthetics should be installed at the bottom of the HMA surface – that is where structural bending-related horizontal tensile stress/strain is maximum. Geosynthetics may not delay crack initiation but will effectively inhibit crack propagation. Early work by Brown *et al*. (1985) demonstrated that fatigue life could be increased by up to 10 times using polymer grids as tensile reinforcement in asphalt beams. Further, Brown *et al*. (1985) also noted that, when geogrids were installed in the upper half of asphalt slabs and tested in Nottingham wheel tracking studies, pavement rutting life for a given subgrade vertical strain level could be increased by a factor of 3. Slide C.17 shows much more rutting and cracking observed in an unreinforced slab when compared to almost no rutting visible in the slab with geogrid reinforcement installed at mid-depth (Brown *et al*. 1985). To reduce both HMA fatigue and primary rutting distresses, multiple geogrid installations can be considered, as illustrated in Slide C.18; one at the bottom of the structural HMA layer (i.e. HMA binder course in Slide C.18) and another at the middle of a single HMA layer (or at the bottom of the HMA surface course).

4.2.3. *Reflective cracking mechanism*
Reflective cracking is a major distress type in HMA overlays caused by both environmental and vehicular traffic loads. Premature cracks are typically observed within 2 to 3 years at the surface of the overlay, having the appearance of the cracking/joint pattern that existed in the original pavement. They could be in transverse and longitudinal directions and sometimes appear as reflections on top of patching in the original pavement. Reflective cracking is one of the major failure modes in rehabilitated pavements and is usually overlooked during the overlay design. Water infiltration through reflective cracks can cause both functionally and structurally unsafe pavement surface conditions (see Slides C.20 and C.21). Mitigation of reflective cracking in asphalt pavement overlays calls for a good understanding of the main causes associated with modes of loading: (1) contractions and

expansions of the original pavement components (e.g. slab in the underlying jointed concrete pavement) causing stress concentration in the overlay due to temperature variations, and (2) traffic-load-induced shearing and bending and the related mixed mode stresses causing crack propagation in the overlay, as illustrated in Slides C.22 and C.23 (Baek and Al-Qadi 2009).

4.2.4. *Reflective cracking control measures*

There is a multitude of reflective crack control measures, some of which are referred to as interlayer systems, with targeted functions of waterproofing the crack, resisting high tensile strain in the overlay bottom, and reinforcement to arrest high stress concentration developed at the tips of cracks in the overlay due to movement of the original pavement (see Slides C.25 to C.27). Interlayer systems include: sand asphalt, Stress Absorbing Membrane Interlayer (SAMI), bitumen-impregnated nonwoven geotextile, geomembrane/geocomposite, steel netting, and strain tolerant layer. These systems offer the functions of waterproofing and/or resisting high strain. Especially stiff geogrids and geocomposites, 3D grids, steel netting, and fiberglass grids provide significant reinforcement and serve as a stress absorbing interlayer to arrest crack formation. It is important to note that fiberglass grids need to effectively bond to the bottom of overlay through a tack coat application as indicated in Slides C.27 and C.29. Cleveland *et al*. (2002) studied the effectiveness of different geosynthetics for mitigating reflective cracking using the Texas Transportation Institute (TTI) overlay tester, which accommodated a $75 \times 150 \times 500$ mm HMA beam and evaluated the relative ability of different beams (with and without a geosynthetic) to resist thermal cracking. Fiberglass-grid-reinforced overlays outperformed those unreinforced ones for up to twice as many days in the life of an overlay depending on the overlay thickness and temperature differential.

4.3. Base course mechanical stabilization in paved roads

4.3.1. *Use of geogrids for base course mechanical stabilization*

Geogrids are the types of geosynthetics most frequently used in the road construction industry for mechanical stabilization. Geogrids are commonly used over weak subgrade soils to provide a working platform for construction equipment. Such an application places a geogrid at the subgrade/aggregate interface to increase the bearing capacity or the support of construction equipment over a soft subgrade with CBR less than 3%. Since the aggregate placement as a subbase requires large thicknesses for low subgrade strengths, the subgrade restraint use of geogrid can therefore be quite beneficial by offering a reduced aggregate thickness alternative in unpaved roads.

In thinly paved low to moderate volume roads and thicker airport pavements, unbound aggregate layers serve as major structural components of the flexible pavement system. Geogrids can effectively perform aggregate base course mechanical stabilization by restraining movement of aggregate particles through geogrid-aggregate interlocking (see Slides C.33 to C.35). This is the lateral restraint mechanism which increases horizontal confinement resulting in a higher localized stiffness around the geogrid to ultimately cause a bearing capacity increase in the pavement structure.

4.3.2. *The concept of lateral restraint*

The concept of confinement or 'lateral restraint' is illustrated in the U.S. Army Corps of Engineers document, 'Use of Geogrids in Pavement Construction' (USACE 2003). Slide C.36 presents a figure from this document showing the primary geogrid mechanism as defined by the USACE. Simply stated, lateral restraint is a unique characteristic of geogrid stabilization as the particle 'strike-through' (i.e. particle presence in geogrid apertures) results in confinement of the aggregate during loading, leading to an increase in stiffness of the aggregate-geogrid composite material. This stiffness enhancement leads to an improvement of both vertical and horizontal stress distribution, resulting in a reduced maximum pressure being applied to the pavement subgrade.

Through the interlock between the geogrids and aggregate, geogrids are assumed to have higher friction and confining stresses than the smoother surfaced geotextiles. This is in part due to the additional bearing resistance created in the geogrid ribs as aggregate particles provide the interlock in the geogrid apertures. When placed in a granular base course, geogrids, through interlocking, may restrain the lateral spreading of the granular base layer, thereby developing a relatively 'stiffer' layer surrounding the geogrid. Interlock is essential to the performance of any geogrid in mechanical stabilization (see Slides C.37 to C.40).

On the interlock between the geogrid and aggregate particles, Jewell *et al*. (1984) identified early on the important mechanisms of soil and geogrid interactions through the use of large shear box testing. Seven granular soils associated with a biaxial geogrid with an aperture width of 17.3 mm were tested. Direct shear tests for the various soil gradations adopted indicated that the granular soil particle size and gradation compared to the geogrid aperture size had an influence on the size of the shear zone. The research findings of Jewell *et al*. (1984) therefore laid down the foundation for understanding the fundamental mechanisms by which geogrids reinforce/stabilize pavement systems by introducing the idea of choosing the type of geogrid for the intended aggregate particle sizes and gradation.

Mechanically Stabilized Layers (MSLs) with geogrid enhance resilient modulus, provide more uniform support for the surface course, and better control and limit long-term permanent deformation accumulation. Base course mechanical stabilization with geogrid ensures its successful and beneficial application in low to moderate volume roads having thin hot-mix asphalt (HMA) surfaces and subgrade CBRs between 3 and 8%. In addition to potentially reducing shear deformation in aggregates, the control of aggregate movement, especially in the upper part of the layer adjacent to the HMA, may

also reduce HMA fatigue distress. Hence, a geogrid interlayer can typically be used to reduce the overall thickness of a pavement system for a target design life or extend the design life of the pavement (see Slides C.41 to C.44).

4.3.3. *Quantification of pavement system improvement*
The improvement to the pavement system provided by base stabilization, using geogrid or other geosynthetics, is frequently quantified by ratios such as TBR or BCR. Traffic Benefit Ratio (TBR) is the ratio of (1) the number of load cycles on a geosynthetic mechanically stabilized section to reach a defined failure state to (2) the number of load cycles on a non-stabilized section, with the same geometry and material constituents, to reach the same defined failure state, say a certain rut depth along the wheel paths. TBR is sometimes termed Traffic Improvement Factor (TIF). On the other hand, Base Course Reduction (BCR) is the percent reduction in the mechanically stabilized base, or subbase, thickness from the non-stabilized section, with the same material constituents, to reach the same defined failure state and pavement life. It should be noted that both TBR and BCR definitions come from the era of the most commonly used empirical pavement design procedures, such as the 1993 AASHTO flexible pavement design based on the AASHO Road Test, which took place in Ottawa, Illinois in 1958–1960 (Slides C.48 and C.49). (AASHO was renamed as AASHTO in 1973.)

In Section 3 of the AASHTO R50-09 document (AASHTO 2013), also referred to as 'designation PP46', entitled, 'Geosynthetic Reinforcement of the Aggregate Base Course of Flexible Pavement Structures', AASHTO states that, 'because the benefits of geosynthetic reinforced pavement structures may not be derived theoretically, test sections are necessary to obtain benefit quantification'. In Section 5 of the same document, it is stated that design procedures 'use experimentally derived input parameters that are often geosynthetic specific' and 'users of this document are encouraged to affirm their designs with field verification of the reinforced pavement performance'. In the same document, AASHTO later states that 'traffic benefit ratio (TBR) and base course reduction (BCR) are the parameters that need to be quantified through full-scale testing'. In other words, the AASHTO R50-09 (PP46) document provides guidance to specifiers on required research needed to generate design values and a design process, and requires product-specific performance-based design values to be obtained from constructed field test sections necessary to quantify benefit. Based on the 1993 empirical AASHTO pavement design procedure, structural layer coefficients are modified for mechanically stabilized layers with geosynthetics through the introduction of LCR = Layer Coefficient Ratio (enhanced layer coefficient).

Slides C.52 to C.55 demonstrate the application of the LCR concept in flexible pavement design examples when enhanced AASHTO layer coefficients are assigned to a granular base stabilized with a geogrid. For the same base thickness, geogrid mechanical stabilization increases the structural capacity quantified by the Structural Number (SN) of the pavement. Alternatively, for a target SN, geogrid mechanical stabilization can provide base course reduction when geogrid is placed at the bottom of the base layer. It should be noted that the most important factor used in the design examples here is the enhanced layer coefficient influenced by the level of mechanical stabilization provided by the geogrid. A quantification of geogrid mechanical stabilization, resulting in an increase of local stiffness near the geogrid, is key to establishing the enhanced layer coefficient.

In the Mechanistic-Empirical (M-E) pavement design methodology, pavement performance is no longer linked only to pavement thicknesses and loading conditions. Instead, performance is characterized by failure linked to a critical pavement response, such as shear stress in the upper part of the subgrade, which can be responsible for subgrade pavement rutting failure. Proper modeling of pavement materials and the reinforcement and stabilization mechanisms is essential to obtain accurate response prediction under applied wheel loading. The effectiveness of geogrid in the base stabilization application can then be quantified by means of a 'Response Benefit' from the geogrid. Therefore, an appropriate M-E design approach for the case of geogrid base stabilization could be achieved by lowering critical pavement responses.

4.4. UIUC mechanistic model for base mechanical stabilization

4.4.1. *Presentation of the model*
To help quantify the effectiveness of geogrid mechanical stabilization, a finite element (FE) program was developed at the University of Illinois at Urbana-Champaign (UIUC) to properly analyze flexible pavements with geogrid-stabilized base considering nonlinear, stress-dependent behavior of unbound aggregate base and subgrade layers (Kwon *et al*. 2005). The axisymmetric FE model developed in line with the Level I analysis of the nationwide Mechanistic-Empirical Pavement Design Guide (MEPDG) effort in the United States considers the directional dependency of load-induced stiffening (anisotropic modulus properties) of the granular base materials and the compaction and preloading-induced residual stresses in the base course. However, by varying the geogrid tensile strength/stiffness and adjusting the modulus of the membrane element representing geogrid in the FE model, no appreciable geogrid response benefit could be quantified. When a geogrid was placed at the bottom of the base layer, no reduction in vertical deviator strains on top of subgrade could be achieved, which may be due to the limiting continuum behavior assumed in the granular base and the assumed full bonding at the base-subgrade interface. Further, when unrealistically high geogrid modulus properties (approximately 10 times higher than typical values from experiments) were assigned to the membrane element, reduced subgrade deviator strains could only be computed in the FE analysis (see Slides C.59 to C.61). Yet, geogrid stabilization of base course has been well established to increase base stiffness through lateral restraint and better distribute

the wheel load over subgrade to lower subgrade critical responses.

4.4.2. *Validation of the model*

Attempts were made to validate the UIUC mechanistic FE model results using pavement responses to accelerated loading from full-scale pavement testing (Al-Qadi *et al*. 2006, 2008b). Testing conducted at the University of Illinois focused on evaluating the effectiveness of geogrids on the response and performance of low-volume flexible pavements constructed on low strength subgrade (i.e. CBR = 4%). Nine instrumented pavement sections were designed and constructed to measure pavement responses and monitor pavement performance. All pavement sections consisted of an HMA layer underlain by an unbound aggregate base resting on a compacted/prepared subgrade. These pavement sections were heavily instrumented with pressure cells, linear variable differential transformers (LVDTs) and strain gauges to measure the pavement response to moving wheel load during testing, and with thermocouples, time domain reflectometer (TDR) probes and piezometers to capture environmental changes during testing. The variables considered in the study included HMA and granular base layer thicknesses, and the type and location of geogrid within the granular base course. Most of the geogrid-stabilized sections had the geogrid placed at the base-subgrade interface, except for the thicker sections (457 mm aggregate base layer thickness) which also had geogrid layers placed in the upper portions of the base layer (see Slides C.62 to C.66).

Testing was conducted using the mobile Accelerated Transportation Loading ASsembly (ATLAS) for response and trafficking data collection in the UIUC Advanced Transportation Research and Engineering Laboratory. In general, analyses of measured responses indicated that the no-geogrid control sections had higher tensile strains measured at the bottom of the HMA, higher vertical pressure and resilient deformation at the top of the subgrade, and significantly greater lateral deformations in the aggregate base layer; especially in the direction of traffic, compared to the sections with geogrid-stabilized base. This observation was further validated by the measured surface rutting. It was evident that the aggregate-geogrid interlock reduced both the lateral strain in the aggregate layer and the vertical deformation of the pavement surface. At the end of trafficking, the no-geogrid control sections exhibited more pronounced pavement distresses including greater surface rutting due to subgrade shear failure as well as aggregate lateral movement. The effectiveness of geogrid in confining the aggregate was evident in the relatively thick granular base layer when the geogrid was placed within the upper part of the base layer (see Slides C.69 to C.79).

Dynamic cone penetrometer (DCP) tests were conducted along non-trafficked areas on each section immediately after testing to estimate thicknesses and the in situ bearing capacities of the base and subgrade materials. Slide C.80 shows the number of DCP blows needed to penetrate through the base into the subgrade in non-trafficked pavement test section locations (Kwon and Tutumluer 2009). Changes in slopes of the straight lines indicate variation in strength. The higher number of blows required in the sections with geogrid-stabilized base shows the stronger behavior of the stabilized base compared to the no-geogrid base. In addition, the DCP results indicated a non-uniform 'modulus' throughout the base layer, as well as intermixing of the base aggregate and weak subgrade soils, which was observed at various levels after section excavation. Similar stiffening effects near the installed geogrid locations in base courses were also observed from DCP testing in actual pavement projects, such as the one from a California highway site indicated in Slide C.81 (Kwon and Tutumluer 2009).

4.4.3. *Discrete element modeling*

Micromechanics-based modeling approaches such as the Discrete Element Method (DEM) could provide an explanation for the behavior of the pavement with geogrid-stabilized base. Results from a DEM approach, which considers actual geogrid geometries and aggregate interlock, also suggest that the incorporation of geogrid in unbound materials causes 'stiffening' of the surrounding area. Such important research findings by the ITASCA Group in Germany and the University of Nottingham in the UK focused on modeling this effect using the three-dimensional Particle Flow Code (PFC3D) DEM program (Konietzky *et al*. 2004; Konietzky and Keip 2005; McDowell *et al*. 2006). Their work presented in Slides C.82 and C.83 identified a relatively higher modulus zone developed around the geogrid due to aggregate interlock and locked-in permanent residual stresses. The calculated residual stresses could be directly linked to the increased confinement around the geogrid. It should be noted that the extent of the mobilized residual stress areas depends on the characteristics of the aggregate and geogrid.

The mechanistic model validation efforts involved comparing the outcome of the FE model to the field data obtained from the full-scale tests. The aggregate-geogrid interlock mechanism from the DEM findings was linked to the continuum analysis technique to improve the FE based analysis methodology. It was evident that, when base course anisotropy and compaction-induced residual stresses were considered in the analyses, the main trends in response behavior were in better agreement with those measured in the field. Slide C.90 shows contour plots of predicted modulus distributions in the entire base and subgrade layers with residual stresses used as initial conditions in the base course (see Slide C.87). In this FE modeling approach, an increase in horizontal confinement due to residual stresses can result in significant increases in the moduli of the base and subgrade layers in the vicinity of the geogrid reinforcement. This behavior agrees with the DEM results.

The benefits of including geogrids in the pavement system could be successfully modeled by considering residual stress concentrations assigned in the geogrid-aggregate vicinity. Such residual stresses assigned in the vicinity of the geogrid, as previously shown by the DEM studies, considerably increased the resilient moduli

predicted in the base and subgrade of the modeled pavement section. As listed in Slide C.91, this resulted in lower vertical pressure on subgrade, less vertical deflection at top of subgrade and lower aggregate longitudinal deformation in the geogrid-stabilized base sections. Furthermore, the predictions were in good agreement with the measured responses from the full-scale tests (Kwon *et al*. 2009).

4.4.4. *Summary on the UIUC mechanistic model*
In summary, test pavements with geogrid-stabilized base constructed over CBR = 4% subgrade exhibited: (i) lower vertical pressure on top of subgrade; (ii) less vertical deflection at subgrade interface when tested at low speed; (iii) higher strength/stiffness properties in the vicinity of geogrid; (iv) less longitudinal aggregate displacement in the base; and (v) less accumulated permanent deformation in pavement sections. Major benefits of M-E geogrid base mechanical stabilization design can be listed as follows: (1) lower critical pavement responses were predicted by the UIUC mechanistic model linked to longer pavement life and (2) realistic quantification of the aggregate interlock was responsible for stiffness enhancement. It should be noted that traditional FWD testing cannot detect this local geogrid-aggregate mechanism. When analyzing pavement sections with geogrid-stabilized base, residual stresses induced by initial compaction can be assigned in the vicinity of the geogrid layer to properly assign higher modulus properties in the stiffened zones and base course sublayers. (Base course sublayers are further discussed in Section 4.6.1)

4.5. How to quantify level of stiffening due to geogrid-aggregate interlock

4.5.1. *Relevant properties of aggregate and geogrid*
Lateral restraint is a primary mechanism of geogrid base stabilization contributing to the performance improvement of flexible pavements, and the interlocking between the geogrid and aggregate is responsible for the stiffness enhancement in a zone formed around the geogrid. The current problem with evaluating aggregate-geogrid interlock and the effectiveness of currently available geogrid products is that there is no representative laboratory test to quantify the stiffness enhancement provided by the interlock in the geogrid-aggregate composite system. For example, for unbound aggregates, the properties that seem to be influential may include gradation, angularity, hardness, density, and surface texture/friction as outlined by Giroud (2009), highlighted in Slide C.93. For a geogrid, the properties that can have a great influence on performance include aperture size and geometry, junction strength, rib shape, and rib stiffness (Giroud 2009).

4.5.2. *Quantification of relevant aggregate properties*
Besides the grain size distribution, aggregate shape properties, especially the flat and elongated (F&E) ratio, the angularity index (AI), and the surface texture (ST) index, are key indices quantified by the Enhanced University of Illinois Aggregate Image Analyzer (E-UIAIA) (Tutumluer *et al.* 2000; Rao *et al*. 2002; Moaveni *et al*. 2013). Representative samples of granular materials for base course in pavements or ballast in railroad tracks are typically scanned and analyzed using the recently enhanced E-UIAIA to determine the values of the F&E ratio, AI, and ST index, which can be used as the essential morphological data to generate ballast particle shapes as three-dimensional (3D) polyhedrons (i.e. individual discrete elements utilized in the ballast DEM models – see Slide 94). These aggregate particles generated for the assembly deformation behavior in DEM simulations are typically rigid individual elements to match the gradation and shape properties quantified from sieve analysis and E-UIAIA.

4.5.3. *Discrete Element Method (DEM) to model geogrid-aggregate interlock*
As mentioned earlier, the Discrete Element Method (DEM) is one of the most suitable numerical approaches to simulate a granular system that consists of discrete particles. The DEM simulation approach developed at the University of Illinois adopts real polyhedral particles and has the capability to create actual aggregate particles as 3D polyhedron elements having the same particle size distributions and imaging quantified average shapes and angularities. This DEM approach was calibrated by the laboratory large scale direct shear test results for ballast size aggregate application (Tutumluer *et al*. 2006) and has been successfully utilized to simulate complex ballast behavior, such as: effects of multi-scale aggregate morphological properties, gradation, and fouling (Tutumluer *et al*. 2006, 2007 2008, 2009). A successful field validation study was also completed to conclude that the DEM approach was quite adequate and reasonably accurate for predicting actual ballast layer deformation behavior (Tutumluer *et al*. 2011).

4.5.4. *Tests on the geogrid-aggregate composite system*
In Slides C.95 to C.97, ongoing research at the University of Illinois is described for quantifying the benefits of geogrid-stabilized railroad ballast on the shear strength and permanent deformation behavior from large-scale triaxial testing in the laboratory. With the capability to create actual ballast aggregate particles as 3D polyhedron elements having the same particle size distributions and imaging quantified average shapes and angularities, the DEM simulations were able to capture the ballast behavior with and without geogrids reasonably accurately (Qian *et al*. 2013b, 2018).

The bender element test, commonly carried out for the evaluation of shear modulus of soils through shear wave propagation, may provide an additional way to study the geogrid-aggregate composite system. The bender element which has optimal coupling with soils and compatible operating frequency is widely used as a shear wave transducer (Lee and Santamarina 2005). Lee and Santamarina (2007) monitored the shear wave velocities during sand liquefaction by using a series of bender elements horizontally installed at different levels in a sand specimen. A similar setup was used by Byun and Tutumluer (2017) who introduced a novel application of

bender elements as shear wave transducers for quantifying local stiffness increase in the vicinity of a geogrid (see Slides C.98 to C.104). It should be noted that shear modulus is estimated at small-strain level, while resilient modulus is estimated at larger-strain levels (Sawangsuriya *et al*. 2005). Since the shear modulus estimated at small-strain level decreases with an increase in the strain level, the shear modulus at small-strain should be greater than the resilient modulus at larger strain. The bender elements successfully enabled the periodic monitoring of shear waves for the evaluation of local stiffness, without any disturbance of the aggregate specimen.

Several triaxial test specimens of a dense-graded granite type aggregate were prepared at two different moisture contents for resilient modulus testing (Byun and Tutumluer 2017). Stabilized specimens included a punched-and-drawn triaxial geogrid placed at specimen mid-height. Two pairs of bender elements installed at two different heights on the membrane that wraps around the specimen enabled the measurement of shear waves horizontally across the specimen. Shear wave velocities and axial resilient strains were recorded under the applied stress states. The test results show that the resilient moduli of stabilized specimens were similar to those of the non-stabilized ones tested at the same moisture content. In contrast, the shear moduli obtained at mid-height of stabilized specimens were always greater than those obtained from non-stabilized specimens thus clearly indicating a local stiffness increase in the vicinity of the geogrid. Further, in stabilized specimens, the shear moduli obtained near the upper end were always less than those obtained from the specimen mid-height. The small-strain shear modulus determination by bender elements was quite effective for evaluating the stiffness enhancement provided by geogrid-aggregate interlock (Byun and Tutumluer 2017).

4.6. Mechanistic analysis approach for base course stabilization in paved roads

4.6.1. *Layer stiffness profiles*

The current approach to consider geosynthetic base stabilization in flexible pavement analysis is through establishing mechanically stabilized layer stiffness profiles within the base course as sublayers in an elastic layered pavement system. This was recently presented as recommended practice for incorporating geogrids in Mechanistic-Empirical (M-E) pavement design (see Slides C.113 to C.119 by Vavrik, Applied Research Associates, presented on July 26, 2018). The base layer subdivision accounts for the mechanically stabilized zones of geogrid influence and lateral confinement. Three distinct impact zones were recommended as fully confined, partially confined and unconfined zones with confined zones above and below the geogrid in the case when geogrid is installed within the base layer and above the geogrid only when geogrid is installed at the subgrade-base interface. The sublayers are assigned with enhanced modulus properties based on fully confined and partially confined mechanical stabilization levels due to the interaction of aggregate and geosynthetics. How to determine the enhanced modulus properties of the mechanically stabilized zones in the proximity of geosynthetics is still posed as a research question in this approach (see Slide C.117). Furthermore, as indicated in Slides C.118 and C.119, pavement damage or distress models, also known as transfer functions in the context of M-E design approach, need to be calibrated for various pavement failure criteria (e.g. rutting and cracking) to determine improved layer deterioration rates due to the mechanically stabilized base performance, which is predicted to undergo much lower deformation and modulus degradation trends with applied traffic levels. A three-stage calibration process involving laboratory testing, accelerated pavement testing, and full-scale field test conditions is suggested for full consideration in the development of transfer function re-calibration.

4.6.2. *Quantification of stiffness enhancement*

As an application of the approach described above, Byun *et al*. (2018) presented findings from a recent laboratory study which could successfully quantify local stiffness enhancement of aggregates through micromechanical interlocking provided by two different types of geogrids and applied these findings in the modeling of the resilient response characteristics of geogrid-stabilized base course composite systems (see Slides C.109 to C.111). Their work considered the mechanically stabilized layer stiffness profiles as sublayers in an elastic layered pavement system modeling. Using three pairs of bender elements as shear wave transducers, the horizontal stiffness profiles were determined above mid-heights of aggregate specimens where two types of geogrids with square and triangular shaped apertures were installed. For the two geogrid types, the shear modulus profiles estimated from shear wave measurements decreased as the distance from the geogrid location increased. The stiffness increase near the geogrid with the triangular aperture was greater than that near the geogrid with square aperture. Considering the variations in shear moduli with distance from the geogrid location, the local stiffness enhancements provided by the two geogrid types were quantified as percent increases in various stiffened zones above the geogrid, in line with the concept of mechanical stabilization and stiffening of the pavement unbound aggregate base. Accordingly, increased resilient moduli–in comparison to base course moduli of non-stabilized pavements (i.e. control pavements)–were assigned to sublayers of a constructed geogrid-stabilized aggregate base course layer for conducting flexible pavement mechanistic analysis and modeling.

4.6.3. *Benefit of stiffness enhancement on pavement life*

According to Byun *et al*. (2018), at the bottom of the HMA layer, lower tensile stresses and strains were predicted in the horizontal direction for the two geogrid-stabilized pavement sections compared to those for the non-stabilized pavement. The lower HMA tensile strains would imply longer pavement life with respect to fatigue cracking. At mid-depth of the base layer, larger confinement and horizontal compressive stresses were

predicted for the geogrid-stabilized pavement sections compared to those for the non-stabilized pavement (Byun *et al*. 2018). Finally, on top of the subgrade, lower vertical deviator stresses and strains were predicted for the geogrid-stabilized pavement sections than those for the non-stabilized pavement. Like in the HMA fatigue case, the lower vertical deviator stresses and strains would correspond to longer pavement life with respect to rutting.

4.7. Concluding remarks for geosynthetic-improved paved roads

The following concluding remarks can be made for the use of geosynthetics for improvement of paved roads:

- When used as asphalt concrete or hot-mix asphalt (HMA) surface layer reinforcement, geosynthetics can increase pavement fatigue life by delaying crack formation, reduce asphalt rutting, and strengthen overlays to reduce reflection cracking.
- By providing paved road mechanical stabilization, geosynthetics offer significant benefits for extending pavement life and allowing reduced thickness of unbound aggregate base and/or subbase layers.
- Geosynthetic design can be empirical or preferably Mechanistic-Empirical (M-E).
- The current M-E approach to consider geosynthetic base stabilization in flexible pavement analysis is through establishing mechanically stabilized layer stiffness profiles within the base course as sublayers in an elastic layered pavement system.
- Recent promising research offers ways to quantify the magnitude and extent of the enhanced stiffness zone in sublayers of granular base and subbase for M-E design.

M-E design should be calibrated based on laboratory testing, large-scale testing, accelerated pavement testing, and based on performance trends of monitored field test sections. Enhanced modulus assignments in base and subbase layers need to be coordinated with the re-calibration efforts for the currently used transfer functions.

5. RELEVANCE OF TESTS AND TRIALS TO REAL ROADS

5.1. Introduction

The author of this Section 5 of the paper represents a geogrid manufacturer, which has been heavily involved in research into and development of the use of geogrids to improve the performance of granular layers in roads for more than 30 years, and the aim of this section is to share some of that experience. The material presented concentrates on mechanical stabilization, but tensioned membrane is also addressed. The main subjects are unpaved roads which are principally granular or aggregate-surfaced, and the granular part provides most of the load carrying capacity.

Trafficking trials and other forms of repeated load testing are the most common ways of developing data to verify calculation models and create pavement design methods taking the benefits of geosynthetics into account, but there are two common questions. Firstly, is the difference in performance between, say, a control road section and a section incorporating a geosynthetic, due solely to the presence of the geosynthetic? Secondly, because a trial road pavement is inevitably arranged to reach a terminal condition relatively quickly, is its performance relevant to real in-service roads? These are important considerations and the main aim of this section is to look at these two questions.

5.2. The empirical nature of road pavement design

The AASHTO (1993) Guide for the Design of Pavement Structures (AASHTO 1993) described in Section 4 of this paper was based on the AASHO Road Test (HRB 1961). The AASHO Road Test was carried out in the late 1950s and early 1960s in Ottawa, Illinois, USA and some of the test details are summarized in Slides D.4 to D.9. The AASHO Road Test was composed of six loops or test tracks, with both asphalt and concrete pavement sections built over a fat clay subgrade. The loops were trafficked by a variety of heavy vehicles, reaching about 1 million ESALs. The data gathered from the AASHO Road Test were used as the basis for a number of design methods given in a series of versions of the AASHTO Guide, up until the last one published in 1993. The design method for asphalt pavements was developed as a nomograph which provides a solution based on the various input parameters. The method was also expressed as a formula, as presented on Slides D.10 and D.11. Slide D.12 provides reminders about the units to be used in the formula.

The main reason for summarizing the AASHO Road Test is to make the important point that the resulting design method is 100% empirical, based on observing the performance of the test sections, resulting in a design relationship. This is common with most pavement design methods, which rely to some extent on observations of actual performance in order to develop a design algorithm or relationship. It is therefore a logical step that, when developing a design method for pavements which takes into account the benefits of mechanical stabilization provided by a suitable geosynthetic, then this should also be done by observing the results from trafficking trials and loading tests.

5.3. The concept of road index (RI)

There are many publications providing results from trafficking trials and cyclic plate loading tests, for a wide variety of pavement layer arrangements and supporting subgrade soils. Some of these trials are summarized in Section 5.4. It was considered useful to be able to assign a single value to any pavement section which would take account of all the main variables. The proposal was the Road Index (or RI). Road Index is defined as follows:

$$RI = 10 \times D \times CBR^{0.5} \quad (11)$$

where D is thickness of a subbase in meters and CBR in % relates to the supporting subgrade. This expression is of a similar form to the design equation for unpaved roads with no geosynthetic published by Giroud and Noiray (1981), which is given in Slide D.14. It has been rearranged with both main variables on the right-hand side, and with CBR to the power of 0.5 rather than 0.63. Further explanation of RI is given in Slide D.15 and a method of taking different pavement materials into account based on an equivalence approach is given in Slide D.16. The reason for including the factor 10 is to give simple numbers to one decimal place for the resulting index values. RI is therefore related to performance but is not intended for use in design and should be quoted to one decimal place only. The scale of RI is approximately logarithmic (e.g. an increase of RI from, say, 4.0 to 5.0 corresponds approximately to a tenfold increase in design number of ESALs). RI is only intended to provide an index for comparing pavement sections which are mainly granular.

The application of RI is illustrated with reference to design charts for granular pavements (consisting of unbound granular base and subbase, with chip seal or thin asphalt surfacing up to a maximum bound thickness of 40 mm) published in Austroads (2017) as outlined in Slides D.18 to D.20. The chart in Slide D.19 provides a simple method of determining total granular thickness based on the design traffic and subgrade CBR. The upper part of the total thickness should be a high-quality base course material. The chart in Slide D.19 may be extended to lower traffic volumes by adding the low volume road design chart (also published in Austroads 2017) to the left side, as seen in Slide D.20. This results in a design relationship suitable for numbers of ESALs between 1000 and 10^9. Slide D.21 shows how the RI definition relates to the combined charts for subgrade CBR = 2%. RI values for higher subgrade CBR are also shown. In order to get similar RI for various CBR values at any specific value of ESAL, it was found necessary to use a power 0.5 in Equation (11) as mentioned above. It may be seen that, for low volume roads, RI is in the range 5.0 to 7.0, whereas for high volume roads RI is from 7.0 to 14.0. RI is indicated for all trial pavements described in the sections which follow.

5.4. Trafficking trials and the importance of isolating variables

5.4.1. *Overview of trafficking trials*

The table in Slide D.23 gives a summary of notable trafficking trials which have been carried out over the last 30 years (references to all trials are given in Slides D.130 and D.131). The table includes various important features of each trial: inclusion of surfacing, total plan area, the type of trial and method of trafficking, and whether or not it was covered – namely protected from weather by a shelter. The maximum number of ESALs reached is given, the largest being 800 000. However, it should be noted that the US Army Corps of Engineers (USACE) trial of 1991 listed second in the table reached 10 000 passes of a single 130-kN wheel, which would represent more than 800 000 ESALs. The information given in the table indicates a wide range of trial conditions.

5.4.2. *Aims of a trafficking trial*

What are the ideal aims of a trafficking trial? This is illustrated in Slides D.24 and D.25, which make the simple point that, if the target of a trial is to establish the benefit of the presence of a geogrid at the base of the granular layer, then all other properties in the two sections should be identical. If any other properties differ between the two sections, then this adds uncertainty and the need to compensate for these additional differences as part of the interpretation process. Some differences are unavoidable, for example, it is not possible to construct two adjacent pavements with identical thicknesses, but they should be as close as possible, and such differences should be known and taken into account in back-analysis (which is illustrated in Section 5.7).

5.4.3. *Measurement of parameters and importance of consistency*

The results of many trafficking trials are used to illustrate various points in the sections which follow, all arranged in a similar way, with the number of passes or loadings on the x-axis, and a measure of rutting on the y-axis. Slide D.26 illustrates the two main methods used to define rut measurement: rut depth, also called 'apparent rut' (measured from the highest point of the deformed road surface to the bottom of the rut) and deformation, also called 'elevation rut' (measured from the initial road surface to the bottom of the rut). The difference between the two is the heave.

The importance of minimizing the effects of unwanted variables has been stressed above, and is illustrated in the paragraphs which follow, looking firstly at the aggregate itself and then secondly at the subgrade.

5.4.4. *Consistency of granular layer*

Slides D.27 to D.32 show the results of an investigation carried out to quantify the importance of consistency of the granular component of a trial road pavement. This work was carried out using a laboratory trafficker, which is a small-scale device as shown in Slides D.27 and D.28. Laboratory traffickers have the disadvantage that their small-scale results are in doubt about the relevance of the measured data to actual pavements, but they have some advantages too. Firstly, the volumes of pavement material being prepared are very small, and secondly, a large number of trials can be done over a short period of time making them ideal for investigating variables. Slide D.29 shows the grading envelope of material referred to as 'Type 1 subbase' in UK practice (where the spelling 'sub-base' is used). The envelope is quite wide, so material bought 'off the shelf' could have a wide range of grading, and therefore, performance. This can be seen in Slide D.30, which shows three trafficking results where the only difference is the actual grading of the material delivered from the supplier. Slide D.31 looks at the difference in

behavior due to high and low fines content, both gradings being inside the required envelope. Based on this investigation, it was decided that the graded material delivered directly from the supplier could not be relied on, so a grading was carefully manufactured, by combining materials from different controlled sources, which then resulted in far more consistent performance as shown in Slide D.32, such that a precise grading was adopted as shown in Slide D.33.

5.4.5. *Consistency of subgrade*

Subgrade properties and consistency are also very important when minimizing unwanted variables. Trials carried out by the Transport Research Laboratory (TRL) in the UK are included as the last item in the table in Slide D.23, and their layout is described in Section 5.5. These trials were carried out in a covered area with relatively small test panels. The procedure for these trials is described in detail by Cook *et al*. (2016). Slide D.34 shows a typical panel being prepared. This was done carefully by conditioning a heavy plastic clay (London Clay) to give a CBR as close as possible to 2% after placement. This was checked by an extensive array of penetrometer tests as shown in Slides D.35 and D.36, which confirm the consistent conditions achieved even though several tonnes of clay were being prepared for each trial. This can be compared to the Tostedt 1 trial (Vollmert 2016), also included in the table on Slide D.23. Slide D.37 shows the glacial till subgrade being placed during preparation of the Tostedt 1 trial. This material is a clay-silt-sand mixture, so highly susceptible to water ingress. The Tostedt 1 trial area was large and outdoors, so not sheltered from the weather. Further details are given in Slide D.38. Slides D.39 to D.41 show profiles of data measured during the Tostedt 1 trial along its entire length. The upper profile shows the distribution of subgrade strength in terms of CBR, whereas the lower profile summarizes the main trafficking results in terms of surface deformation at various stages during the trial. The target for the Tostedt 1 trial was a uniform CBR, but it varied from around 1% to over 3%. The lower diagram shows a profile of surface deformation along the Tostedt 1 trial at three stages during the trafficking. Variability is also large, and comparison of the upper and lower profiles does indicate reasonable correspondence between low CBR and large surface deformation and *vice versa*. Slide D.42 has been prepared from the previous slide but only showing trafficking data where they are reasonably uniform over a distance along the trial of 4 m or greater. Slide D.43 then shows these trafficking data against mean CBR for each section based on directly measured CBR values only. This provides a reasonable basis for assessing the Tostedt 1 trial. However, a great deal of uncertainty remains.

The distribution and variability of subgrade properties in the TRL and Tostedt 1 trials illustrate the importance of consistent subgrade preparation. Slides D.44 and D.45 summarize the geotechnical characteristics of the two materials and the major differences are clear both in terms of grading and plasticity. This demonstrates that using large areas of low plasticity subgrade material in trials carried out without a shelter, namely outdoors, is likely to result in major variability of the prepared subgrade. Independent guidance may be found in the reports shown in Slide D.46 (Berg *et al*. 2000; Saeed and Hall 2003).

5.5. Performance limits which define mechanical stabilization

5.5.1. *Mechanical stabilization*

Section 2.1.2 describes how a geosynthetic performs the mechanical stabilization function when it is used to confine a soil material laterally at multiple locations, thereby creating a composite material with a high modulus and restraining displacement of this material. The TRL trials, which were carried out between 2000 and 2013, provide an extensive database of trafficking information which may be used to examine the performance of unpaved roads, in particular the performance limits which should be achieved in a trafficking trial such that mechanical stabilization may be assumed to be the dominant function.

5.5.2. *Description of TRL trials*

Slide D.49 shows the general arrangement of all the TRL trials (Jenner *et al*. 2002), in which a standard axle load was applied along a fixed wheel path over an unpaved road consisting of 300 mm of subbase supported by a plastic clay subgrade with CBR = 2%. The wheel load is therefore perfectly channelized, which can be considered as the most severe pattern of trafficking. Slides D.50 and D.51 show the typical arrangement of a section of the trial consisting of three test panels, where each panel might include a different geosynthetic or might be a control panel without any geosynthetic. Slide D.52 summarizes all eight trials and from the total of 93 test panels, 16 were control panels whereas 77 included a geosynthetic. All panels had the standard arrangement of a 300 mm thick subbase over a subgrade having a CBR of 2%, except for 5 panels of different thicknesses. The standard arrangement has RI = 4.2, which represents a low volume road. The procedure used to control subgrade CBR is described in Section 5.4, while Slide D.53 shows the nature of the subbase material used. The principal performance parameters measured were surface rut depth and deformation during the process of trafficking, as defined in Slide D.26 and shown in Slide D.54, followed by subgrade deformation which was only measured after excavation of the pavement at the end of each trial, as shown in Slide D.55.

5.5.3. *Performance of the trial panels*

Slides D.56 to D.61 summarize the performance of three panels in one of the trials, comprising a control panel and two panels with geosynthetics at the subgrade/subbase interface, consisting of a welded geogrid and a punched-and-drawn geogrid. The slides form an animation showing pavement shape at different stages, and by the end of the trial, there are clear differences in performance. The control panel reaches excessive rutting very quickly, whereas both panels with geosynthetics perform better.

However, it is seen that, whereas the stronger welded geogrid is tending towards tensioned membrane behavior, the punched-and-drawn geogrid has created sufficient confinement to ensure that the geogrid and aggregate behave together as a composite material resulting in mechanical stabilization.

5.5.4. *Surface modulus*

The modulus of a road pavement is frequently determined by analyzing the results of surface plate load testing. This modulus is therefore an overall value, reflecting the contribution from all layers within the zone of influence of the applied load, and is referred to here as the surface modulus. As shown in Slide D.62, surface modulus testing was carried out before each TRL trial using the falling weight deflectometer (FWD) apparatus and occasionally by surface plate loading tests. This testing demonstrated that initial surface modulus is not influenced to any significant extent by the absence or presence of the geosynthetic. Slide D.63 summarizes surface modulus test results from various trials by plotting the measured values against the RI value for the pavement (see Section 5.3 for definition of RI). There is a good correlation as might be expected, but examination of the TRL controls and TRL triaxial (geogrid) results confirms that the presence of a geosynthetic does not affect the surface modulus of the layered system as measured on first-time loading. This behavior is examined and discussed further in Section 5.6.3.

5.5.5. *Performance parameters*

Examination of the 186 final profile shapes measured in the TRL trials suggested that a simple classification system could be used to define the terminal shapes by assigning one of the five definitions described in Slide D.65 (Cook *et al*. 2016). Although partly subjective, the five shape categories are logical and are defined graphically using specific profiles in Slides D.66 to D.71. Slide D.72 provides a summary of the terminal trafficking performance parameters which should be achieved in order to define the performance as mechanical stabilization, in terms of shape and surface deformation. The shape categories CON and CON- (see Slides D.70 and D.71 e.g.) should be achieved. One further important indicator of adequate composite performance was found to be the rate of surface deformation, which should be around 1 mm per 1000 passes or less. These performance limits are considered suitable for unpaved roads. Actual surface deformation and rate of deformation would be considerably less for paved roads where mechanical stabilization is functioning adequately.

5.6. Various trafficking trials and tests

5.6.1. *Scope of this section*

This section summarizes the results from three trafficking trials (all included in the table in Slide D.23) and one cyclic plate load test program. In each case, various types of geosynthetics were included and the performance of a control section was compared to the performance of sections with a geosynthetic. Triaxial geogrids (as illustrated in Slide D.74) were included in all four test programs and the comparisons discussed below concentrate on the performance of this form of geosynthetic. Each case includes additional variables or components, covering a wide range of performance. References of publications describing the trials and tests can be found in Slides D.130 and D.131.

One of the variables of relevance in each trial and test is the actual applied load, defined either as an axle load or the load applied to a test plate in the case of surface load testing. The load applied to a test plate is intended to represent the load applied by one side of an axle. Accordingly, the load applied to a test plate is typically half of an axle load. In most cases, the axle load is 80 kN, which is the Equivalent Single Axle Load (ESAL) defined in AASHTO (1993), and the load applied to a test plate is 40 kN. In the case of testing by the US Army Corps of Engineers (USACE) described in Section 5.6.4, the axle load was 89 kN. In this situation the number of passes of the actual axle load is converted into number of passes of the ESAL using an equivalence relationship as discussed above in Section 1.2.3, and also in Slides D.75 and D.76.

5.6.2. *Montana Phase 2 (2012)*

The Montana trafficking trials were carried out by the Western Transportation Institute, Montana State University (Cuelho *et al*. 2014). The Phase 2 trafficking trial is well known and has been reported extensively, with a summary provided in Slide D.78. The unpaved road trial area was large and was trafficked outdoors by a real truck with the aim of creating channelized wheel loading. Maximum number of ESALs reached was about 900. RI is 3.3 for this pavement (Slide D.79), which is low and consistent with the small number of ESALs achieved. Various geosynthetics were used in the trials, including two grades of triaxial geogrids. Slide D.80 shows how trafficking results in rapid accumulation of surface deformation with a terminal rate in the order of 100 mm per 1000 passes, which is far from the limits required for mechanical stabilization to be the dominant mechanism as established in Section 5.5.

Verification of the trafficking performance observed in Montana Phase 2 is provided by comparison with the results from one of the TRL unpaved road trials. With reference to Slide D.52, which summarizes the program of trials carried out by TRL (see Section 5.6.3), there were five test panels in Trial No. TRL6 with non-standard thicknesses (the standard thickness of TRL test panels was 300 mm). One of these panels was built 250 mm thick over a triaxial geogrid, as described in Slides D.82 and D.83. Side-by-side comparison in Slides D.84 and D.85 shows the 250 mm thick section on the left and a 'standard' TRL 300 mm thick section on the right, both with a triaxial geogrid present at the base. The difference in performance is major, illustrating the effect of reducing subbase thickness by 50 mm. The RI of the 250 mm thick TRL section is 3.7, which is similar to the RI value of 3.3 related to Montana Phase 2 (275 mm thick). The trafficking diagram in Slide D.86 combines the results

for both trials, showing that the performance seen in Montana Phase 2 would be expected.

The behavior of the 250 mm thick section seen in Slide D.85 is rapidly degenerating into tensioned membrane, which is only applicable to unpaved roads with channelized traffic where large surface deformations are tolerable (see Section 2.2.4). This behavior is not relevant to paved roads or permanent unpaved roads for which deep ruts are not acceptable. This is seen in Slide D.86 where trafficking in both Montana Phase 2 (275 mm thick) and the 250 mm TRL trial do not reach the lower ESAL limit for low volume road design according to Austroads and certainly not at an acceptable surface deformation.

5.6.3. *Transport research laboratory (2000 to 2013)*
The Transport Research Laboratory (TRL) trials included some test panels with triaxial geogrids. These are described by Cook *et al*. (2016) and are illustrated in Slides D.87 to D.89. The basic trial arrangement is the same as described in Section 5.5.2. The side-by-side comparison of terminal performance of the non-stabilized control panel top left of Slide D.92 and the same pavement cross section incorporating a triaxial geogrid on the top right of Slide D.92 provides an illustration of the potential for mechanical stabilization to influence the performance of the granular layer in an unpaved road carrying channelized wheel loading. The performance of the mechanically stabilized panel meets in every way the performance limit requirements given in Slide D.72. Importantly, it can be seen that mechanical stabilization has resulted in retention of the thickness and shape across the full width of the aggregate/geogrid composite. Slide D.93 presents the same data against the background of the Austroads design charts, confirming a performance relevant to low volume permanent roads, and therefore suitable for providing empirical data to form the basis of a design method for permanent roads.

The graph in Slide D.93 includes the initial surface modulus of both test panels, which are essentially the same, as is trafficking performance for the first 20 to 30 ESALs. Therefore, although the conditions to create mechanical stabilization are established at the time of placement and compaction of the aggregate around and into the apertures of the geogrid, the benefit in terms of enhanced surface performance (both surface stiffness and rut depth) only becomes evident as the trafficking progresses. This is the normal trend observed in most trafficking trials of this type, as summarized in Slide D.63 in terms of surface modulus. Further evidence is presented in Slides D.94 and D.95 in terms of the early behavior during trafficking. The data summarized in Slide D.94 are based on the 88 standard (300 mm subbase over subgrade with CBR = 2%) test panels trafficked during the eight TRL trials. The graph shows the rut depth at various stages in each trial (25, 50, 100 and 200 passes) plotted against final rut depth. Therefore, each trial is represented by a row of dots moving up the diagram as trafficking progresses, and the two arrows indicate the trials presented in Slide D.93. For each set of data in Slide D.94 an equation is given representing the linear regression of the data. The data for 25 passes are close to being a horizontal line, meaning that after 25 passes there is no indication of the likely eventual behavior of the pavement section. This pattern gradually changes and, by 200 passes, there is a clear relationship between the achieved rut depth and the final rut depth. Slide D.95 shows the same relationships for surface deformation, and a similar trend is evident, although there are no data available for 25 passes.

5.6.4. *US Army Corps of Engineers Phase 1 (2012)*
The US Army Corps of Engineers (USACE) Phase 1 trial is described by Jersey *et al*. (2012) and illustrated in Slides D.96 to D.102. The important differences compared to the TRL trials are that a thin asphalt layer is included in the pavement section (resulting in RI = 7.6), and the trafficking is not channelized, but arranged to have a lateral wander pattern as the tandem wheels are run over the trial sections. This can be seen in Slide D.98 where the wheels may be set to run anywhere within the black trafficking zone in the top left inset photograph. The main result is shown in Slide D.100, comparing the trafficking performance of the control section with that of the same section including a triaxial geogrid in the granular base layer. A second comparative section is shown in which a thicker asphalt layer was used compared to the control section. The difference in performance between the control section and the mechanically stabilized pavement is clear and is illustrated in Slide D.101 in relation to the Austroads design charts. The performance of this pavement, in terms of number of ESALs reaching 100 000 passes and surface deformation being limited to 12 mm, is appropriate to road pavements of this class and is consistent with RI = 7.6. This performance is relevant to the design of real in-service pavements, and the back-analysis of this trial is presented in Section 5.7.

Slide D.102 shows the control section and mechanically stabilized pavements side-by-side after an excavation had been made through the pavements following completion of trafficking. Rather like the TRL comparison in Slide D.92, the benefit of using a mechanically stabilized aggregate base course is clear. The thickness and shape of the stabilized base course in the pavement on the right of Slide D.102 have been retained for the full 100 000 ESALs, whereas in the control section on the left of Slide D.102 there is massive loss of aggregate thickness in the wheel-path with lateral migration of aggregate resulting in increased thickness in the heaved part of the pavement. This mobility of the aggregate has occurred because it is not mechanically stabilized, in contrast to the pavement on the right of Slide D.102.

5.6.5. *Louisiana Transportation Research Center cyclic plate testing (2014)*
The Louisiana Transportation Research Center (LTRC) cyclic plate testing program, described by Abu-Farsakh *et al*. (2015), illustrates the effect of additional variables as shown in Slide D.104. The test pavement includes an asphalt surfacing layer, supported by a base layer which is 450 mm thick. There are three test sections as illustrated in Slide D.104 with different arrangements of the

aggregate base layer: a non-stabilized control section, a section with a single triaxial geogrid and a section with two layers of triaxial geogrid. Slide D.105 shows the cyclic load test arrangement approximately to scale. Slide D.106 shows the surface deformation – that is directly under the test plate – versus the number of load cycles, which is indicated as number of ESALs because the applied load was 40 kN, which is similar to the load applied by one end of a standard 80 kN axle. The performance approaches 4×10^6 ESALs with only 12 mm surface deformation, which is representative of permanent pavement performance and consistent with RI = 8.5. It can be seen that Section 2 with two layers of triaxial geogrid outperforms both Section 3 with a single layer of triaxial geogrid and Section 4 which is the control section.

Further insight into this performance is gained by examining the permanent deformation at different levels in the pavement section. Deformation was also measured at the top of the base course and the top of the subgrade. Slide D.107 presents the data for the control section, noting that the surface deformation scale on the y-axis has been changed to enable the behavior to be seen more clearly. The vertical differences between the three traces indicate the loss in thickness of the base and asphalt layers. In both cases they are significant. Slide D.108 shows the same data for the single geogrid section, whereas Slide D.109 shows the same data for the double geogrid section. It may be seen that, although the single geogrid layer does reduce both losses in base course thickness and overall deformation, the double geogrid layer results in almost zero loss in base thickness and a consequential substantial reduction in surface deformation. This is indicating that the second geogrid layer is necessary to ensure that the mechanical stabilization benefit is present over the full 450 mm depth of the base course.

This observation fits in well with the concept shown in Slide D.110, namely that there is a limit to the extent above (or below) a geogrid over which the benefit of mechanical stabilization is likely to be present. Clearly it does not extend indefinitely, and the scheme in Slide D.110 indicates a fully confined zone adjacent to the geogrid, then a partially confined transitional zone extending to the point where mechanical stabilization is no longer effective. Based on trafficking studies, large shear-box tests and large triaxial tests, the distance between the geogrid and the point where mechanical stabilization is no longer effective has been established to be about 300 mm for typical road building aggregate, although the maximum extent of the fully confined zone may be about 150 mm. This is further substantiated by the results from the LTRC cyclic plate load testing program described above.

5.6.6. *Summary of trafficking trials and tests*

Slides D.111 to D.115 summarize all four test programs discussed above on a single rut depth versus ESAL graph (see Slide D.112), which also indicates the RI for each pavement section. As RI becomes higher, the maximum ESAL achieved also becomes higher. Slide D.113 includes a data-point at a specific rut depth on each plot, and then in Slide D.114 the matching control section behavior for each of the trials is shown. The length of each horizontal bar, when expressed as a ratio, has a specific term, the TBR (traffic benefit ratio, defined in Section 4.3.3). The calculated values are plotted in Slide D.115 for each trial. The TBR considers the contribution of all layers in the pavement section, so, in the case of USACE and LTRC tests, a TBR cannot be assigned solely to the contribution of the aggregate layer. The TBR values become lower as the asphalt layer makes a larger contribution to the overall pavement performance. The Montana trial result has a small TBR, but this is because the dominant mechanism is tensioned membrane, which has a relatively small effect on trafficking performance.

5.7. Interpretation of the stabilization factor from a trafficking trial

Slides D.116 to D.121 contain the full back-analysis of a trial (the USACE Phase 1 trial described in Section 5.6.4) using the AASHTO 1993 design method for asphalt pavements, in order to establish quantitatively the benefit of mechanical stabilization on the granular base course layer. The basis for this interpretation is given in Slide D.117, where it is indicated that an additional term is included in the calculation of the structural number of the base layer (base layer in this case, but it could equally well be applied to the subbase), designated as f_{SN}, or 'factor on the structural number' for that layer. This is synonymous with the Layer Coefficient Ratio (LCR) term often mentioned in this situation. The layer coefficient is the 'a' value, however the benefit could equally well be interpreted as applying to the layer thickness, so that f_{SN} is preferred and illustrated pictorially in Slide D.118. Slide D.119 indicates the two match points which have been chosen to compare the number of ESALs obtained in both the control and stabilized sections, in this case at 12.5 mm rut depth.

Slide D.120 gives the full interpretation procedure in a tabulated form. All known parameters are given for both the control and stabilized pavement sections, and then each interpreted value is indicated by a superscript $^{(1)}$, $^{(2)}$, and so on. Each step is described in detail in Slide D.121 and can be summarized as follows: start with the control section, and then, using the AASHTO formula, adjust the resilient modulus of the subgrade (M_r) by trial-and-error until the calculated number of ESALs matches that measured. It is then necessary to create an imaginary 'adjusted' control section, which is a control section with the same layer thicknesses and subgrade properties as the stabilized section. Based on the measured subgrade properties of both sections, M_r established previously for the control section is adjusted pro-rata to obtain M_r for the stabilized and adjusted control sections. The number of ESALs for the adjusted control is then calculated using the AASHTO formula based on the adjusted SN values. In the stabilized section, the SN of the base layer (SN_{base}) is adjusted by trial-and-error until the number of ESALs matches the observed value. The value of f_{SN} is then found as the ratio of SN_{base} values comparing the stabilized value to that of the adjusted control. Importantly, this procedure

has taken account of the small differences in layer thicknesses and subgrade parameters between the control and the stabilized sections. In this example, $f_{SN} = 2.14$.

5.8. Automated plate load test

The automated plate load test (APLT) has been developed to permit investigation and verification of mechanical stabilization in situ, by D. White (previously of Iowa State University). The device is shown in Slides D.123 and D.124, consisting of a self-ballasted trailer which houses all the required loading, control and recording equipment. A plate is lowered onto the pavement surface, which is then cyclically loaded. Automation of the testing and recording processes greatly reduces the time required to carry out tests. A comparative result is shown in Slide D.126 for a relatively thin unpaved road trial (Slide D.125), comparing the permanent surface deformation for three cases: control section, mechanically stabilized layer using biaxial geogrid, and the same with triaxial geogrid. Permanent deformation on the first cycle is much the same in each case, but the differences become clear by the end of the 250 cycles recorded. This is consistent with earlier observations from trafficking trials, namely that initial surface modulus and trafficking induced deformations are similar over the first few passes or cycles, but the difference, and therefore the benefit due to mechanical stabilization in terms of surface modulus and deformation, is only seen after a substantial number of passes or loadings have taken place. This is also seen in Slide D.127 which compares resilient modulus based on results from several studies.

5.9. Concluding remarks for relevance of tests and trials

Concluding remarks are given in Slides D.128 and D.129, and are repeated here:

(*a*) Pavement design is empirical so that cyclic plate loading tests and trafficking trials are required in order to assess the benefits of adding geosynthetics to the granular layers.
(*b*) The Road Index (RI) is a simple concept for comparing different unpaved and paved roads.
(*c*) The planning and execution of trafficking trials should minimize the effect of unwanted variables.
(*d*) Features such as very large test areas, testing outdoors and using low plasticity subgrades are likely to contribute to unwanted variations in test parameters.
(*e*) The extensive series of TRL trials have provided target minimum terminal performance parameters which help determine if the prevalent mechanism is mechanical stabilization.
(*f*) A wide variety of tests and trafficking trials provide data to help establish design methods for both unpaved and paved roads taking account of the benefits of mechanical stabilization, however it is required that the behavior exhibited in the trial or test is also mechanical stabilization.
(*g*) An example of deriving a stabilization factor from a trial has been presented.
(*h*) APLT is a technique which gives further insight into the behavior of unpaved and paved roads which incorporate geosynthetics.

6. CONCLUSION

As discussed in this paper, the mechanisms involved in the behavior of a road are now well understood, and the functions performed by geosynthetics in these mechanisms are now well established.

Design methods are available that take into account the benefits brought by geosynthetics in both unpaved and paved roads. These design methods are constantly improved thanks to the fact that research is very active in this field. Theoretical studies, laboratory-scale studies, and field studies are combined to improve existing methods and develop new design methods that quantify more accurately the contributions of geosynthetics.

Several types of geosynthetics are currently used in roads. It can be expected that new innovative geosynthetics will periodically appear on the market, which will open up new possibilities and, at the same time, require more research to develop new design methods.

Regardless of future developments, it is clear from this paper and the presentations that appear in the Supplemental Material to this paper that, today, thanks to existing geosynthetics, it is possible to design and construct roads with a better performance and longer service life than without geosynthetics, or, alternatively, for a given service life, roads that are less expensive.

NOTATION

Basic SI units are given in parentheses.

AI	Angularity Index (degrees)
a	half-length of the chord of the deflected geotextile (m)
B	width of tire contact area (m)
BCR	Base Course Reduction (dimensionless)
CBR	California Bearing Ratio (dimensionless)
c_u	undrained shear strength of subgrade (Pa)
D	thickness of subbase (m)
E_{bc}	modulus of the base course (Pa)
ESAL	Equivalent Single Axle Load, which is not actually a load but a number of axle passes (dimensionless)
E_{sg}	modulus of the subgrade (Pa)
F&E	Flat and Elongated Ratio (dimensionless)
f_s	serviceability limit for the apparent rut depth at the surface (m)
h	base thickness (m)
h_0	unreinforced base thickness under a static load (m)
h_r	reinforced base thickness under a static load (m)
J	aperture stability modulus (m×N/°)
J_g	geotextile tensile stiffness (N/m)
L	length of tire contact area (m)

LCR	Layer Coefficient Ratio (dimensionless)
MIF	Modulus Improvement Factor (dimensionless)
M_r	resilient modulus of subgrade (Pa)
m	bearing capacity mobilization factor (dimensionless)
N	number of load cycles (dimensionless)
N_{actual}	number of passes of the actual axles (dimensionless)
N_c	bearing capacity factor (dimensionless)
n	constant calibrated with field data (dimensionless)
P	wheel load (N)
P_a	axle load (N)
P_{actual}	actual axle load (N)
P_{standard}	standard axle load (N)
p_i	maximum vertical stress on top of the subgrade (Pa)
q_u	bearing capacity of subgrade soil (Pa)
RI	Road Index (dimensionless)
r	radius of tire contact area (m)
s_a	apparent rut depth at the surface, defined as the vertical distance between peak and valley of the deformed road surface (m)
s_e	elevation rut depth, defined as the vertical distance between the initial elevation of the road surface and the elevation of the rut bottom, at the interface between base and subgrade (m)
SN	Structural Number (dimensionless)
ST	Surface Texture Index (dimensionless)
TBR	Traffic Benefit Ratio (dimensionless)
TIF	Traffic Improvement Factor (dimensionless)
α	stress distribution angle from the base to the subgrade (°)
α_0	stress distribution angle for a uniform medium (°)
α_1	stress distribution angle for $N = 1$ (i.e. static loading) (°)
Δh	reduction of base thickness (m)
ε_g	geotextile tensile strain (dimensionless)
λ	distribution angle reduction rate (dimensionless)
ξ	constant calibrated with field data (dimensionless)
ρ	factor to correlate undrained shear strength and CBR of subgrade (Pa)
ω	constant calibrated with field data (dimensionless)

ABBREVIATIONS

AASHO	American Association of State Highway Officials
AASHTO	American Association of State Highway and Transportation Officials
AC	Asphalt Concrete
APLT	Automated Plate Load Test
ASTM	American Society for Testing and Materials
ATLAS	Accelerated Transportation Loading ASsembly
DCP	Dynamic Cone Penetrometer
DEM	Discrete Element Method
E-UIAIA	Enhanced University of Illinois Aggregate Image Analyzer
FE	Finite Element
FHWA	Federal Highway Administration of the United States
FWD	Falling Weight Deflectometer
HMA	Hot Mix Asphalt
LTRC	Louisiana Transportation Research Center
LVDT	Linear Variable Differential Transformer
M-E	Mechanistic Empirical
MEPDG	Mechanistic-Empirical Pavement Design Guide
MSL	Mechanically Stabilized Layer
PCC	Portland Cement Concrete
RAP	Reclaimed Asphalt Pavement
SAMI	Stress Absorbing Membrane Interlayer
TDR	Time Domain Reflectometer
TRL	Transport Research Laboratory
TTI	Texas Transportation Institute
UIUC	University of Illinois at Urbana-Champaign
USACE	United States Army Corps of Engineers

REFERENCES

AASHTO (1990). *Task Force 25 Report — Guide Specifications and Test Procedures for Geotextiles. Subcommittee on New Highway Materials.* American Association of State Transportation and Highway Officials, Washington, DC, USA.

AASHTO (1993). *Guide for Design of Pavement Structures*, American Association of State and Highway Transportation Officials, Washington, DC, USA.

AASHTO (2013). *Standard Practice for Geosynthetic Reinforcement of the Aggregate Base Course of Flexible Pavement Structures.* American Association of State and Highway Transportation Officials, Washington, DC, USA. AASHTO R50-09.

Abu-Farsakh, M., Hanandeh, S., Chern, Q. & Mohammed, L. (2015). Evaluation of geosynthetic reinforced/stabilized pavement built over soft subgrade soil using cyclic plate loading testing. In *Proceedings of Geosynthetics 2015*, Portland, Oregon, USA. Industrial Fabrics Association International (IFAI), Roseville, MN, USA, pp. 823–829.

Al-Qadi, I. L., Tutumluer, E. & Dessouky, S. (2006). Construction and instrumentation of full-scale geogrid-reinforced flexible pavement test sections. In *Airfield and Highway Pavements, Proceedings of the ASCE Transportation and Development Institute (T&DI) Airfield and Highway Pavement Specialty Conference, April 30-May 3, 2006*, Atlanta, Georgia, Al-Qadi, I. L., Editor, American Society of Civil Engineers, Reston, VA, USA, pp. 131–142.

Al-Qadi, I., Morian, D., Stoffels, S., Elseifi, M., Cehab, G. & Stark, T. (2008a). *Syntheses on Use of Geosynthetics in Pavements and Development of A Roadmap to Geosynthetically-Modified Pavements*, Federal Highway Administration, Washington, DC, USA.

Al-Qadi, I. L., Dessouky, S., Kwon, J. & Tutumluer, E. (2008b). Geogrid in flexible pavements: validated mechanism. *Transportation Research Record, Journal of the Transportation Research Board*, **2045**, 102–109.

Anderson, R. P. (2006). Geogrid separation. *Proceedings of International Conference on New Developments in Geoenvironmental and Geotechnical Engineering, 9-11 November*, University of Incheon, Incheon, Republic of Korea.

ASTM (2015). D7864/D7864M - 15 Standard test method for determining the aperture stability modulus of geogrids. ASTM, West Conshohocken, PA, USA.

ASTM (2016). D1883 – 16 Standard test method for california bearing ratio (CBR) of laboratory-compacted soils. ASTM, West Conshohocken, PA, USA.

ASTM (2017). D 4595 – 17 Standard test method for tensile properties of geotextiles by the wide-width strip method. ASTM, West Conshohocken, PA, USA.

Austroads (2017). *Guide to Pavement Technology: Part 2: Pavement Structural Design*, Austroads Publication AGPT02-12, Austroads Ltd, Sydney, Australia, 283p.

Baek, J. & Al-Qadi, I. L. (2009). Reflective cracking: modeling fracture behavior of hot-mix asphalt overlays with interlayer systems. *Journal of the Association of Asphalt Paving Technologists*, **78**, 638–673.

Barenberg, E. J., Hales, J. & Dowland, J. (1975). *Evaluation of Soil-Aggregate Systems with MIRAFI Fabrics*, UILU-ENG-75-2020 Report for Celanese Fibers Marketing Company. University of Illinois, Urbana, IL, USA.

Bathurst, R. J. & Naftchali, F. M. (2021). Geosynthetic reinforcement stiffness for analytical and numerical modelling of reinforced soil structures. *Geotextiles and Geomembranes*, **49**, No. 4, 921–940.

Berg, R. R., Christopher, B. R. & Perkins, S. (2000). *Geosynthetic reinforcement of the Aggregate base/subbase courses of pavement structures. GMA White Paper II*, Geosynthetic Materials Association, Roseville, MN, USA, 176p.

Brown, S. F., Brunton, J. M., Hughes, D. A. B. & Brodrick, B. V. (1985). Polymer grid reinforcement of asphalt. *Journal of Asphalt Technology*, **54**, 18–41.

Burmister, D. M. (1958). Evaluation of pavement systems of the WASHO road test by layered systems method. *Bulletin*, **177**, 26–54.

Byun, Y. H. & Tutumluer, E. (2017). Bender elements successfully quantified stiffness enhancement provided by geogrid–aggregate interlock. *Transportation Research Record, Journal of the Transportation Research Board*, **2656**, 31–39.

Byun, Y. H., Qamhia, I., Tutumluer, E. & Wayne, M. H. (2018). Geogrid-stabilized Aggregate base stiffness: laboratory characterization and modeling for mechanistic pavement analysis. *Proceedings of the IS-Atlanta Symposium, Geomechanics From Micro to Macro in Research and Practice, Jointly Organized by ISSMGE TC105 and TC202, September 10-12, 2018*, Atlanta, Georgia.

Christopher, B. R. & Holtz, R. D. (1989). *Geotextile Design and Construction Guidelines. Participant Notebook*, Report No. FHWA-HI-90-001. Federal Highway Administration, National Highway Institute, Washington, DC, 311p.

Cleveland, G. S., Button, J. W. & Lytton, R. L. (2002). *Geosynthetics in Flexible and Rigid Pavement Overlay Systems to Reduce Reflection Cracking*, Report No. FHWA/TX-02/1777-1. Texas Transportation Institute, College Station, Texas, USA, 298p.

Cook, J. D., Dobie, M. J. D. & Blackman, D. I. (2016). The development of APT methodology in the application and derivation of geosynthetic benefits in roadway design. In *Conference on The Roles of Accelerated Pavement Testing in Pavement Sustainability: Engineering, Environment, and Economics*, Aguiar-Moya, J. P., Vargas-Nordcbeck, A., Leiva-Villacorta, F. & Loría-Salazar, L. G., Editors, Springer International Publishing, Switzerland, pp. 257–275.

Cuelho, E., Perkins, S. & Morris, Z. (2014). *Relative Operational Performance of Geosynthetics Used as Subgrade Stabilisation*, Report FHWA/MT-14-002/7712-251. Western Transportation Institute, Montana State University, Bozeman, MT, USA, 313p.

Deacon, J. A., Fin, F., Hudson, W., Obrcian, V. D., Hindermann, W., Warden, W. & Monismith, C. (1969). Load equivalency in flexible pavements. *Proceedings of the Association of Asphalt Paving Technologists*, **38**, 465–494.

Gabr, M., (2001). *Cyclic Plate Loading Tests on Geogrid Reinforced Roads. Research Report*. Tensar Earth Technologies, Inc., Raleigh, NC, USA.

Giroud, J. P. (1977). *Les Géotextiles.* Le Moniteur des Travaux Publics et du Bâtiment, No. 51, Paris, France, pp. 61–67, (in French).

Giroud, J. P. (2009). An assessment of the use of geogrids in unpaved roads and unpaved areas. *Proceedings of the Jubilee Symposium on Polymer Geogrid Reinforcement*, Institution of Civil Engineers, London, UK, pp. 23–36.

Giroud, J. P. (2010). Development of criteria for geotextiles and granular filters. *Terzaghi Lecture Summary, Proceedings of the 9th International Conference on Geosynthetics,* May 2010, Guarujá, Brazil, Vol. 1, pp. 45–64.

Giroud, J. P. & Han, J. (2004a). Design method for geogrid-reinforced unpaved roads. I development of design method. *Journal of Geotechnical and Geoenvironmental Engineering*, **130**, No. 8, 775–786.

Giroud, J. P. & Han, J. (2004b). Design method for geogrid-reinforced unpaved roads. II calibration and applications. *Journal of Geotechnical and Geoenvironmental Engineering*, **130**, No. 8, 787–797.

Giroud, J. P. & Noiray, L. (1981). Geotextile-reinforced unpaved road design. *Journal of the Geotechnical Division*, **107**, No. GT 9, 1233–1254, with discussion and closure, Vol. 108, No. GT 12, December 1982, pp. 1654-1670.

Guo, J. (2018). *Evaluation and Design of Wicking Geotextile for Pavement Applications.* Ph.D. dissertation, the University of Kansas, Lawrence, KS, USA.

Guo, J., Han, J., Zhang, X. & Li, Z. (2019). Evaluation of moisture reduction in aggregate base by wicking geotextile using soil column tests. *Geotextiles and Geomembranes*, **47**, 306–314.

Hammitt, G. M. (1970). *Thickness Requirement for Unsurfaced Roads and Airfields, Bare Base Support*, Project 3782-65, Technical Report S-70-5. U.S. Army Engineer Waterways Experiment Station, CE, Vicksburg, Mississippi, USA, 135p.

Han, J. & Zhang, X. (2014). Recent advances in the use of geosynthetics to enhance sustainability of roadways. *Invited Keynote Lecture, Conference on Advances in Civil Engineering for Sustainable Development, 27–29 August*, Horpibulsuk, S., Chinkulkijniwat, A. & Suksiripattanapong, C., Editors, Suranaree University of Technology, Nakhon Ratchasima, Thailand, pp. 29–39.

Han, J., Yang, X., Parsons, R. L. & Leshchinsky, D. (2007). *Design of Geocell-Reinforced Bases. Interim Research Report to PRS.* University of Kansas, Lawrence, KS, USA.

Han, J., Zhang, X. & Guo, J. (2018). Improving roadway performance by wicking geotextile to reduce soil moisture. *Proceedings of the University of Minnesota 66th Annual Geotechnical Engineering Conference, February 23*, Minneapolis, MN, USA, Labuz, J. F. & Skiles, J., Editors, pp. 67–81.

Holtz, R. D., Christopher, B. R. & Berg, R. R. (1998). *Geosynthetic Design and Construction Guidelines*, FHWA-NHI-95-038. Course No. 13213, Federal Highway Administration, Washington DC, USA.

Holtz, R. D., Christopher, B. R. & Berg, R. R. (2008). *Geosynthetic Design and Construction Guidelines*, FHWA-NHI-07-092, Federal Highway Administration, Washington, DC, USA, 592p.

HRB (Highway Research Board) (1961). *The AASHO Road Test History and Description of Project*, HRB Special Report 61A. National Academy of Sciences-National Research Council, Publication 816, Washington, DC, USA.

Huang, Y. H. (2004). *Pavement Analysis and Design*, 2nd edn. Pearson, Upper Saddle River, NJ, USA, 792p.

Jenner, C. J., Watts, G. R. A. & Blackman, D. I. (2002). Trafficking of reinforced, unpaved subbases over a controlled subgrade. *Proceedings of the 7th International Conference on Geosynthetics*, Delmas, P., Gourc, J. P. & Girard, H., Editors, Swets & Zeitlinger. Lisse, Netherlands,, pp. 931–934.

Jersey, S. R., Tingle, J. S., Norwood, G. J., Kwon, J. & Wayne, M. H. (2012). Full-scale evaluation of geogrid reinforced thin flexible pavements. *Journal of the Transportation Research Board*, **2310**, No. 1, 61–71.

Jewell, R. A., Milligan, G. W. E., Sarsby, R. W. & Dubois, D. (1984). Interaction between soil and geogrids. *Proceedings Symposium on*

Polymer Grid Reinforcement in Civil Engineering, The Institution of Civil Engineers, London, UK, pp. 19–29.

Koerner, R. M. (1984). *Construction and Geotechnical Methods in Foundation Engineering*, McGraw-Hill, New York, NY, USA.

Konietzky, H. & Keip, M. A. (2005). *PFC3D Discrete Element Modeling of Geogrid Pullout Tests. Interim Progress Report, Prepared for Tensar Earth Technologies, Inc*. ITASCA Consultants GmbH, Gelsenkirchen, Germany.

Konietzky, H., te Kamp, L., Gröger, T. & Jenner, C. (2004). Use of DEM to model the interlocking effect of geogrids under static and cyclic loading. In *Numerical Modeling in Micromechanics via Particle Methods*, Shimizu, Y., Hart, R. & Cundall, P., Editors, A.A. Balkema, Rotterdam, The Netherlands, pp. 3–12.

Kwon, J. & Tutumluer, E. (2009). Geogrid base reinforcement with aggregate interlock and modeling of the associated stiffness enhancement in mechanistic pavement analysis. *Transportation Research Record, Journal of the Transportation Research Board*, **2116**, 85–95.

Kwon, J., Tutumluer, E. & Kim, M. (2005). Development of a mechanistic model for geosynthetic-reinforced flexible pavements. *Geosynthetics International*, **12**, No. 6, 310–320.

Kwon, J., Tutumluer, E. & Al-Qadi, I. L. (2009). Validated mechanistic model for geogrid base reinforced flexible pavements. *ASCE Journal of Transportation Engineering*, **135**, No. 12, 915–926.

Lee, J. S. & Santamarina, J. C. (2005). Bender elements: performance and signal interpretation. *Journal of Geotechnical and Geoenvironmental Engineering*, **131**, No. 9, 1063–1070, https://doi.org/10.1061/(ASCE)1090-0241(2005)131:9(1063).

Lee, J. S. & Santamarina, J. C. (2007). Seismic monitoring short-duration events: liquefaction in 1 g models. *Canadian Geotechnical Journal*, **44**, No. 6, 659–672, https://doi.org/10.1139/t07-020.

Leflaive, E. & Puig, J. (1973). Emploi des textiles dans les travaux de terrassement et de drainage. *Revue Générale des Routes et des Aérodromes*, **43**, No. 493, 73–89, in French.

McDowell, G. R., Harireche, O., Konietzky, H., Brown, S. F. & Thom, N. H. (2006). Discrete element modeling of geogrid-reinforced aggregates. *Proceedings Institution of Civil Engineers, Geotechnical Engineering*, **159**, 35–48.

McGown, A. & Ozelton, M. W. (1973). Fabric membrane in flexible pavement construction over soils of low bearing strength. *Civil Engineering and Public Works Review*, **68**, No. 798, 25–29.

Moaveni, M., Wang, S., Hart, J. M., Tutumluer, E. & Ahuja, N. (2013). Evaluation of aggregate size and shape by means of segmentation techniques and aggregate image processing algorithms. *Transportation Research Record: Journal of the Transportation Research Board*, **2335**, 50–59.

Pokharel, S. (2010). *Experimental Study on Geocell-Reinforced Bases Under Static and Dynamic Loading*. Ph.D. dissertation, the University of Kansas, Lawrence, KS, USA.

Qian, Y., Han, J., Pokharel, S. K. & Parsons, R. L. (2013a). Performance of triangular aperture geogrid-reinforced base courses over weak subgrade under cyclic loading. *Journal of Materials in Civil Engineering*, **25**, No. 8, 1013–1021.

Qian, Y., Mishra, D., Tutumluer, E. & Kwon, J. (2013b). Comparative evaluation of different aperture geogrids for ballast reinforcement through triaxial testing and discrete element modeling. *Proceedings of Geosynthetics 2013 Conference*, Long Beach, California, Industrial Fabrics Association International, Roseville, MN, USA.

Qian, Y., Tutumluer, E., Mishra, D. & Kazmee, H. (2018). Triaxial testing and discrete-element modelling of geogrid-stabilized rail ballast. *Proceedings of the Institution of Civil Engineers: Ground Improvement*, **171**, No. 4, 223–231.

Rao, C., Tutumluer, E. & Kim, I. T. (2002). Quantification of coarse aggregate angularity based on image analysis. *Transportation Research Record, Journal of the Transportation Research Board*, No. 1787, 117–124.

Saeed, A. & Hall, J. W. (2003). *Accelerated Pavement Testing: Data Guidelines. National Cooperative Highway Research Program*, NCHRP Report 512. Transportation Research Board, Washington, DC, USA, 38p and Appendices.

Sawangsuriya, A., Bosscher, P. J. & Edil, T. B. (2005). Alternative testing techniques for modulus of pavement bases and subgrades. In *Geotechnical Applications for Transportation Infrastructure: Featuring the Marquette Interchange Project in Milwaukee, Wisconsin*, Titi, H. H., Editor, American Society of Civil Engineers, Reston, VA, USA, pp. 103–121.

Steward, J., Williamson, R. & Mohney, J. (1977). *Guidelines for Use of Fabrics in Construction and Maintenance of Low-Volume Roads.* USDA, Forest Service, Washington, DC, USA.

Sun, X., Han, J., Wayne, M. H., Parsons, R. L. & Kwon, J. (2015). Determination of load equivalency for unpaved roads. *Transportation Research Record: Journal of the Transportation Research Board*, **2473**, 233–241, https://doi.org/10.3141/2473-27.

Tutumluer, E., Rao, C. & Stefanski, J. (2000). *Video Image Analysis of Aggregates, Final Project Report*, FHWA-IL-UI-278, Civil Engineering Studies UILU-ENG-2000-2015. University of Illinois Urbana-Champaign, Urbana, IL, USA, July.

Tutumluer, E., Huang, H., Hashash, Y. M. A. & Ghaboussi, J. (2006). Aggregate shape effects on ballast tamping and railroad track lateral stability. *Proceedings of the 2006 annual conferences: AREMA 2006 annual conference*, Louisville, KT, USA, American Railway Engineering and Maintenance of Way Association, Lanham, MD, USA.

Tutumluer, E., Huang, H., Hashash, Y. M. A. & Ghaboussi, J. (2007). Discrete element modeling of railroad ballast settlement. *Proceedings of the 2007 annual conferences: AREMA 2007 annual conference*, Chicago, IL, USA, American Railway Engineering and Maintenance of Way Association, Lanham, MD, USA.

Tutumluer, E., Dombrow, W. & Huang, H. (2008). Laboratory characterization of coal dust fouled ballast behavior. *Proceedings of the 2008 annual conferences: AREMA 2008 annual conference*, Salt Lake City, UT, USA, American Railway Engineering and Maintenance of Way Association, Lanham, MD, USA.

Tutumluer, E., Huang, H., Hashash, Y. M. A. & Ghaboussi, J. (2009). AREMA gradations affecting ballast performance using discrete element modeling (DEM) approach. *Proceedings of the 2009 annual conferences: AREMA 2009 annual conference*, Chicago, IL, USA, American Railway Engineering and Maintenance of Way Association, Lanham, MD, USA.

Tutumluer, E., Qian, Y., Hashash, Y. M. A., Ghaboussi, J. & Davis, D. D. (2011). Field validated discrete element model for railroad ballast. *Proceedings of the 2011 annual conferences: AREMA 2011 annual conference*, Minneapolis, MN, USA, American Railway Engineering and Maintenance of Way Association, Lanham, MD, USA.

USACE (2003). *Use of Geogrids in Pavement Construction. Appendix A, ETL 1110-1-189*, US Army Corps of Engineers, Washington, DC, USA.

Vollmert, A. L. (2016). *Serviceability of Geogrid-Reinforced Granular Layers Under Cyclic-Dynamical Loading*. PhD Thesis, Technical University Clausthal, Clausthal, Germany, 259p, (in German).

Wang, F., Han, J., Zhang, X. & Guo, J. (2017). Laboratory tests to evaluate effectiveness of wicking fabric in soil moisture reduction. *Technical Note, Geotextiles and Geomembranes*, **45**, 8–13.

White, D. J., Gieselman, H. H., Douglas, C., Zhang, J. & Vennapusa, P. (2010). *In Situ Compaction Measurements for Geosynthetic Stabilized Subbase: Weirton, West Virginia*, EERC Publication ER10-05. Iowa State University, Ames, IA, USA, 79p.

Zhang, X., Presler, W., Li, L., Jones, D. & Odgers, B. (2014). Use of wicking fabric to help prevent frost boils in Alaskan pavements. *J. Mater. Civ. Eng*, **26**, No. 4, 728–740.

The Editor welcomes discussion on all papers published in Geosynthetics International. Please email your contribution to discussion@geosynthetics-international.com by 15 August 2023.